Deletion of FNDC5/Irisin modifies murine osteocyte function in a sex-specific manner

Anika Shimonty[1], Fabrizio Pin[2], Matt Prideaux[2], Gang Peng[3], Joshua R Huot[2], Hyeonwoo Kim[4], Clifford J Rosen[5], Bruce M Spiegelman[6], Lynda F Bonewald[7*]

[1]Indiana Center for Musculoskeletal Health, School of Medicine, Indiana University, IN, 46202, Indianapolis.

[2]Indiana Center for Musculoskeletal Health, Department of Anatomy, School of Medicine, Indiana University, IN, 46202, Indianapolis.

[3]Indiana Center for Musculoskeletal Health, Department of Medicine and Molecular Genetics, School of Medicine, Indiana University, IN, 46202, Indianapolis.

[4]Department of Biological Sciences, Korea Advanced Institute of Science and Technology, Daejeon, South Korea.

[5]Maine Medical Center Research Institute, ME, 04074, Scarborough, USA.

[6]Department of Cancer Biology, Dana Farber Cancer Institute and Department of Cell Biology, Harvard University Medical School, MA, 02115, Boston, USA.

[7]Department of Anatomy, Cell Biology and Physiology, Orthopaedic Surgery, School of Medicine, Indiana Center for Musculoskeletal Health, Indiana Center for Musculoskeletal Health, Indiana University, IN, 46202, Indianapolis.

***Forcorrespondence:**

lfbonewal@iu.edu(LB)

Abstract

Irisin, released from exercised muscle, has been shown to have beneficial effects on numerous tissues but its effects on bone are unclear. We found significant sex and genotype differences in bone from wildtype (WT) mice compared to mice lacking *Fndc5* (KO), with and without calcium deficiency. Despite their bone being indistinguishable from WT females, KO female mice were partially protected from osteocytic osteolysis and osteoclastic bone resorption when allowed to lactate or when placed on a low-calcium diet. Male KO mice have more but weaker bone compared to WT males, and when challenged with a low-calcium diet lost more bone than WT males. To begin to understand responsible molecular mechanisms, osteocyte transcriptomics was performed. Osteocytes from WT females had greater expression of genes associated with osteocytic osteolysis and osteoclastic bone resorption compared to WT males which had greater expression of genes associated with steroid and fatty acid metabolism. Few differences were observed between female KO and WT osteocytes, but with a low calcium diet, the KO females had lower expression of genes responsible for osteocytic osteolysis and osteoclastic resorption than the WT females. Male KO osteocytes had lower expression of genes associated with steroid and fatty acid metabolism, but higher expression of genes associated with bone resorption compared to male WT. In conclusion, irisin plays a critical role in the development of the male but not the female skeleton and protects male but not female bone from calcium deficiency. We propose irisin ensures the survival of offspring by targeting the osteocyte to provide calcium in lactating females, a novel function for this myokine.

In-text word count (Introduction, Results, and Discussion): 12270

Number of data elements: 1 table, 8 figures.

Introduction

It is widely accepted that bone and muscle interact mechanically as movement of the skeleton by muscle is essential for life. Less well-known but becoming more generally accepted is that muscle and bone can communicate through secreted factors ***Brotto and Bonewald*** (***2015***); ***Bonewald*** (***2019***). Muscle produces factors such as *β*-aminoisobutyric Acid (BAIBA) and irisin with exercise, that have positive effects on bone, adipose tissue, brain, and other organs, whereas sedentary muscle produces factors such as myostatin that has negative effects on both bone and muscle ***Brotto and Bonewald*** (***2015***); ***Karsenty and Mera*** (***2018***); ***Kitase et al.*** (***2018***); ***Bostrom et al.*** (***2012***); ***Hamrick et al.*** (***2006***).

Many of the factors secreted by bone are produced by osteocytes, the most abundant and the longest-living bone cell ***Bonewald*** (***2011***); ***Dallas et al.*** (***2013***). These cells are derived from terminally differentiated osteoblasts that become surrounded by the newly mineralizing bone matrix ***Dallas et al.*** (***2013***). Osteocytes are multifunctional and appear to be the major mechanosensory cell in bone ***Bonewald*** (***2011***); ***Temiyasathit and Jacobs*** (***2010***); ***Uda et al.*** (***2017***). Under unloaded conditions, these cells produce sclerostin, a negative regulator of bone formation and Receptor Activator of Nuclear factor Kappa β ligand (RANKL), the major factor that recruits and activates osteoclasts to resorb bone ***Nakashima et al.*** (***2011***); ***Xiong and O'Brien*** (***2012***); ***Xiong et al.*** (***2015***); ***Ono et al.*** (***2020***). In contrast, with anabolic mechanical loading, these cells produce factors such as prostaglandin E2 (PGE_2) that have positive effects on myogenesis and muscle function ***Mo et al.*** (***2015***). Osteocytes play a major role in mineral metabolism, through regulation of both calcium and phosphate homeostasis. Osteocytes secrete Fibroblast Growth Factor 23 to target the kidney to regulate phosphate excretion. Both Parathyroid Hormone (PTH) and Parathyroid related peptide (PTHrP) regulate calcium homeostasis via the PTH type 1 receptor on osteocytes ***Feng et al.*** (***2009***); ***Teti and Zallone*** (***2009***). Under the physiological calcium-demanding condition of lactation, osteocytes respond to PTHrP by removing their surrounding perilacunar matrix to provide calcium for offspring, and upon weaning this perilacunar matrix is rapidly replaced, a process referred to as perilacunar remodeling ***Qing and Bonewald*** (***2009***); ***Qing et al.*** (***2012***); ***Wysolmerski*** (***2013***). However, under pathological conditions such as ovariectomy, hyperparathyroidism, hypophosphatemic rickets, and cancer, excessive removal of their perilacunar matrix occurs through osteocytic osteolysis ***Tsourdi et al.*** (***2018***); ***Jähn-Rickert and Zimmermann*** (***2021***); ***Pin et al.*** (***2021***); ***Shimonty et al.*** (***2023***).

Bone is the largest calcium reservoir in the body and human mothers can lose an average of 250 mg/day of calcium in milk, emphasizing the need for a calcium-replete diet to prevent bone loss ***Qing et al.*** (***2012***); ***Wysolmerski*** (***2002***); ***Kalkwarf*** (***2004***). During lactation, PTHrP targets the

osteocyte to elevate genes coding for factors necessary for the removal of their calcium-ladened perilacunar matrix and to increase RANKL as an activator of osteoclasts **Kovacs** (**2001**). During lactation, RANKL targets osteoclasts, thereby driving osteoclastic bone resorption. Osteocytic osteolysis is accomplished through the expression of 'osteoclast-specific' genes such as cathepsin K (*Ctsk*), tartrate-resistant acid phosphatase (TRAP, gene *Acp5*), and carbonic anhydrase 1 (*Car 1*) **Qing and Bonewald** (**2009**); **Qing et al.** (**2012**). In addition, there is an increase in genes coding for the proton pumps, ATPase H^+ Transporting V1 Subunit G1 (*Atp6v1g1*) and ATPase H^+ Trans- porting V0 Subunit D2 (*Atp6v0d2*) necessary to dissolve and remove calcium from bone collagen **Jahn** (**2017**).

Systemic calcium deficiency such as a decrease in dietary calcium triggers an increase in PTH, acting to mobilize calcium from bones to maintain normal homeostatic circulating calcium **Goltzman** (**2008**). Worldwide, over 3.5 billion people suffer from dietary calcium deficiency, and women are at a higher risk of this condition **Kumssa et al.** (**2015**); **Body et al.** (**2016**). Aging often results in hypocalcemia and bone loss due to low vitamin D, hypoparathyroidism, genetic abnormalities, medications decreasing dietary calcium absorption, and menopause in women. Calcium deficiency can lead to osteopenia, osteoporosis, and increased fracture risk, primarily due to secondary hyperparathyroidism **Kumssa et al.** (**2015**); **Body et al.** (**2016**).

Irisin is a recently discovered myokine generated in response to exercise when Fibronectin type III Domain Containing protein 5 (FNDC5) is proteolytically cleaved by a yet undetermined protease **Bostrom et al.** (**2012**). FNDC5 is expressed in the heart, kidney, testes, brain, and other tissues; however, skeletal muscle appears to be the primary producer **Erickson** (**2013**); **Maak et al.** (**2021**); **Tsourdi et al.** (**2022**). Cleaved irisin circulates to distant organs, such as adipose tissue where irisin increases a thermogenic gene program, including the expression of uncoupling protein 1 (UCP1) in a process referred to as browning. This is associated with increased energy expenditure and improvement in glucose tolerance, both of which are important for the prevention of Type 2 diabetes and the reduction of complications from obesity **Perakakis et al.** (**2017**); **Korta et al.** (**2019**). Irisin can also regulate glucose uptake in skeletal muscle **Lee et al.** (**2015**), and increases myogenesis and oxidative metabolism, responsible for increasing skeletal muscle mass **Colaianni and Grano** (**2015**). Irisin also plays an important positive role in cognitive functions with exercise, aging, and degenerative diseases such as Alzheimer's disease (AD) and Parkinson's disease (PD) **Islam et al.** (**2021**). Using the tail-vein injection method to deliver exogenous irisin, it was shown that irisin can cross the blood-brain barrier **Islam et al.** (**2021**).

Results from studies regarding the effects of irisin on the skeleton are complex and somewhat contradictory. Colaianni et al have shown that recombinant irisin exerts a beneficial effect on cortical bone in young male mice by reducing the secretion of osteoblast inhibitors and increasing the activity

of osteogenic cells ***Colaianni et al.*** (***2015***). However, another study has shown that recombinant irisin treatment of MLO-Y4 osteocyte-like cells induces gene and protein level expression of *Sost*/sclerostin, a negative regulator of bone formation while maintaining cell viability under oxidative stress ***Kim et al.*** (***2018***). Rosen et al. have shown using female FNDC5 overexpressing female mice that irisin acts directly acts on osteoclast progenitors to increase differentiation and promote bone resorption ***Estell et al.*** (***2020***). Kim et al. have shown that 9-month-old ovariectomized FNDC5 global KO mice are protected against ovariectomy-induced trabecular bone loss through the inactivation of osteocytic osteolysis and osteoclastic bone resorption ***Kim et al.*** (***2018***). The majority of these studies used only male or female mice, suggesting a sex-dependent response may be responsible for these seemingly opposing findings ***Estell et al.*** (***2020***); ***Colaianni et al.*** (***2017***); ***Kawao et al.*** (***2018***); ***Ma et al.*** (***2018***); ***Colucci et al.*** (***2019***); ***Posa et al.*** (***2021***).

As shown previously, FNDC5 deletion has a protective effect against ovariectomy- induced bone loss via a reduction of osteocytic osteolysis and osteoclastic resorption ***Kim et al.*** (***2018***). We, therefore, hypothesized that FNDC5 deletion would also be protective against bone loss due to calcium deficiency that occurs with lactation and a calcium-deficient diet. Our data show that the female skeleton in FNDC5 null female mice was resistant to bone loss due to both lactation and low calcium. However, for FNDC5 null males, deletion not only failed to protect but exacerbated bone loss in response to low calcium. We propose that male and female osteocytes respond to irisin differently under calcium-demanding conditions based on the divergence of the male and female osteocyte transcriptome with sexual maturity when the female osteocyte must serve a critical role in reproduction and lactation.

Results

With lactation, FNDC5 global KO mice lose less bone and are mechanically stronger compared to WT

No significant differences were observed in either bone composition or morphometry between 4-5-month-old virgin WT and FNDC5 global KO female mice (Fig 1A, 1B, 1C, sup table 1), showing that the absence of FNDC5/irisin does not affect female bone development. It has been previously shown that during lactation, maternal bones release calcium to supplement milk, especially in response to the large calcium demand induced by large litter size or a calcium- deficient diet ***Wysolmerski*** (***2002***); ***Ardeshirpour et al.*** (***2015***). Similar to previous studies, 2 weeks of lactation resulted in bone loss in both WT and KO mice, with a significant reduction in cortical bone area (Ct. B.Ar), cortical bone area fraction percentage (Ct.B.Ar/T.Ar%), and cortical thickness (Ct. Th) (Fig 1A, 1B) as well as bone mineral density, BMD (Fig 1C). However, the KO mice lost less bone compared to the WT mice, as evidenced by the significantly higher bone area fraction percent, cortical thickness, and BMD (Fig. 1A, 1B, 1C) as well as the lower percentage of bone loss (Sup Table 1). These data suggest that the FNDC5 KO mice are more resistant to the effects of calcium demand. Analysis of trabecular bone parameters including trabecular bone volume fraction (BV/TV), trabecular thickness (Tb. Th), trabecular spacing (Tb. Sp), and trabecular number (Tb. N) showed no significant difference in bone loss between lactating WT and lactating KO mice (Sup table 1). There was no significant difference in the pup numbers between WT and KO females (Sup fig 1A).

Bone loss can have significant effects on bone mechanical properties including bone strength, stiffness, and fragility. To determine mechanical properties, 3-point bending tests were performed on mice femurs. There was no significant difference between virgin WT and KO mice in terms of ultimate force and stiffness (Fig. 1D). However, femurs from the lactating KO mice were stronger than lactating WT, as evidenced by the higher stiffness and significantly higher ultimate force needed to break the bone (Fig 1D, Sup Table 1, Table 2). This data indicates that lactating KO female bone retains greater resistance to fracture than lactating WT mice by less lactation-induced bone loss.

With lactation, FNDC5 global KO mice have fewer TRAP-positive osteo- clasts and osteocytes as well as smaller osteocyte lacunar area compared to WT mice

Previously it was shown that lactation-induced bone loss occurs via not only osteoclastic bone resorption but also osteocytic osteolysis ***Qing et al*** (***2012***). To determine the relative contribution of each means of resorption, tibial longitudinal sections were stained for tartrate-resistant acid phosphatase TRAP-positive multinucleated osteoclasts as well as TRAP-positive osteocytes.

Virgin FNDC5 KO female mice had fewer TRAP-positive osteocytes compared to virgin WT

mice (Fig. 1E, 1G). This is the first and only difference we have observed between WT and KO female mice and suggests that the osteocytes in the female KO mice are less 'primed' to initiate osteocytic osteolysis. With lactation, TRAP-positive osteocytes significantly increased in both WT and KO mice (Fig 1G, Sup Table 2). Virgin KO mice started with a lower number of TRAP- positive osteocytes compared to virgin WT, and with lactation, their number of TRAP-positive osteocytes was still significantly lower compared to lactating WT (Fig. 1G).

During lactation, in response to calcium demand, osteocytes can remove their perilacunar matrix. This process is similar but not identical to osteoclastic bone resorption ***Tsourdi et al.*** (***2018***); ***Bélanger*** (***1969***); ***Wysolmerski*** (***2012***) as osteoclasts generate resorption pits, whereas osteocytes increase their lacunar size ***Qing et al.*** (***2012***); ***Wysolmerski*** (***2013***). We measured the osteocyte lacunar area and found no significant difference between virgin WT and KO female mice (Fig. 1F, 1H) even though the KO females have fewer TRAP-positive osteocytes (Fig. 1G). With lactation, the lacunar area increased in both groups; however, KO mice had significantly smaller average lacunar area compared to WT (Fig. 1H). We did not observe any difference in the osteocyte density among any of the groups (WT= 258.2±51.46, WT L= 274.6±57.37, KO= 254.8±47.66, and KO L= 273.4±59.75). These data show that female lactating FNDC5 KO mice undergo less osteocytic osteolysis compared to WT females under the calcium-demanding condition of lactation.

In virgin mice, there were no significant differences in osteoclast number per bone perimeter (Oc/B.Pm) between WT and KO female mice (Fig 1I). With lactation, osteoclast number increased in both groups, however, KO mice had significantly fewer osteoclasts (Fig 1I) and a significantly lower percentage increase in the number of osteoclasts compared to WT (Sup Table 1). This suggests that with lactation, fewer osteoclasts are activated in the KO as compared to the WT mice.

RANKL, another major factor in bone resorption ***Xiong and O'Brien*** (***2012***), is also increased during lactation to induce osteoclastic bone resorption ***Ardeshirpour et al.*** (***2015***) by osteocytes, the major source of RANKL ***Nakashima et al.*** (***2011***); ***Xiong and O'Brien*** (***2012***); ***Ono et al.*** (***2020***). Virgin WT and KO mice had comparable serum RANKL levels (Fig. 1J). With lactation, the increase in serum RANKL was significant in the WT mice, but not in the KO mice (Fig. 1I, Sup Table 1).

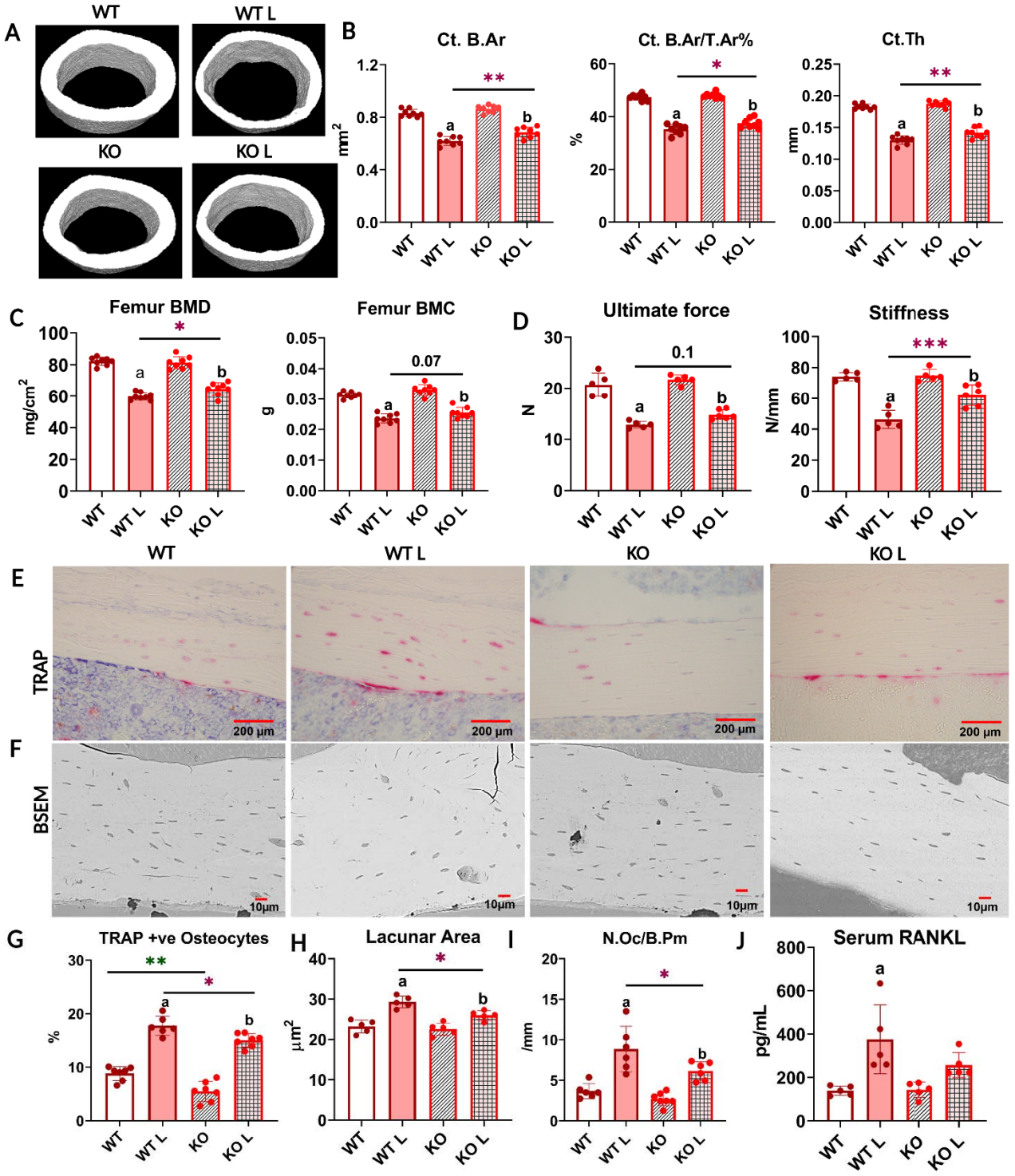

Fig 1: With lactation, FNDC5 global KO mice lose less bone and are mechanically stronger compared to WT

A: Respective μCT images of femoral midshafts from WT virgin (WT), KO virgin (KO), WT lactation (WT L), and KO lactation (KO L) mice.

B: μCT analysis of femoral cortical bone parameters of virgin and lactating WT and KO female mice reported as cortical bone area (Ct. B.Ar), cortical bone area fraction (Ct. B.Ar/ T.Ar %), and

cortical thickness (Ct. Th).

C: Ex vivo DXA analysis for BMD and BMC of femurs from virgin and lactating WT and KO female mice.

D: 3-point bending analysis of WT and KO virgin and lactating mice reported as ultimate force and stiffness.

E: Representative TRAP-stained images of cortical bone from WT virgin (WT), WT lactation (WT L), KO virgin (KO), and KO lactation (KO L) mice.

F: Representative backscatter scanning electron microscope (BSEM) images of WT virgin (WT), KO virgin (KO), WT lactation (WT L), and KO lactation (KO L) mice femur at 400X magnification.

G: Percent TRAP-positive osteocytes (TRAP +ve) in tibia from virgin and lactating WT and KO mice.

H: Osteocyte lacunar area in femurs from virgin and lactating WT and mice.

I: Osteoclast number per bone perimeter in tibia from virgin and lactating WT and KO mice.

J: Serum RANKL levels in virgin and lactating WT and KO mice.

4-5-month-old WT and KO virgin and lactating mice, n= 5-8/group. a= Significantly different from WT, b= Significantly different from KO, *= $p< 0.05$, **= $p< 0.01$, ***= $p< 0.001$. 2-way ANOVA was performed for statistical analysis. The interaction was not significant.

FNDC5 KO female and male bone have opposite responses to a low- calcium diet

After observing that bones are partially protected against lactation-induced bone loss in FNDC5/irisin KO female mice, we sought to determine if FNDC5/irisin null (KO) male bone is protected from calcium deficiency. Therefore, both female and male mice were placed on a calcium-deficient diet for 2 weeks to induce bone loss. We do not see any significant difference in body weight in any of the groups (Sup fig 1B, C), or in food intake (Per day average food intake was 3.9±0.9g for WT females on a normal diet, 3.74±1.01g for KO females on a normal diet, 3.66±1.1g for WT females on a low-calcium-diet, 3.8±0.7g for KO females on a low-calcium-diet, 4.2±1.3g for WT males on a normal diet, 4.3±1.5g for KO males on a normal diet, 3.94±1.8g for WT males on a low-calcium-diet, and 4.4±1.2g for KO males on a low-calcium-diet).

With regards to the female mice, similar results were observed with the low calcium diet as was observed with lactation. At baseline, WT and KO female mice showed no significant differences in their BMD and BMC (Sup Table 2), as well as no differences in either cortical (Fig 2B) or trabecular bone parameters (Sup Table 3). After 2 weeks of a low calcium diet, both WT and KO female mice lost bone as can be evidenced by decreased BMD (Sup Table 2) and bone area fraction (Fig 2B). However, similar to the lactation experiment, the KO female mice were partially resistant to bone loss compared to the female WT mice given a low calcium diet (Fig 2A, B). Interestingly a higher marrow cavity area was observed in the WT compared to the KO, unlike the lactation experiment (Sup Table 2).

Mechanical testing showed that bone from female KO mice required a significantly higher force to break, and thus were stronger com- pared to WT females given a low calcium diet (Fig 2C). Therefore, similar to the calcium-demanding conditions of lactation, on a low calcium diet, the female KO bone is more resistant to bone loss than WT.

Unlike female bone, significant differences were observed between WT and KO male bone at baseline. KO male mice on a normal diet had a significantly higher BMD, BMC (Sup Table 2), and bone area fraction compared to WT males of the same age (Fig 2E). However, femurs from KO mice had significantly lower stiffness than WT (Fig 2F), indicating a difference in the material properties of the bone. Therefore, the KO males have larger, denser, but weaker bones compared to WT males. To determine the effect of calcium deficiency on male mice, KO and WT mice were subjected to a low-calcium diet for 2 weeks. Unlike the female KO mice which were protected from the effects of a low calcium diet, the KO male mice had an opposite response. The male KO mice had greater bone loss compared to the WT male mice (Fig 2D, E, Table 2), the trabecular bone loss followed the same trends but was not statistically significant (Sup Table 2), and the femurs from the KO male mice were significantly less stiff and therefore weaker compared to the WT males on a low calcium diet (Fig 2F). These data confirm a sex-specific response to a low-calcium diet.

To ensure that the effects observed in the KO mice were due to circulating irisin, and not FNDC5 deletion, we injected AAV8- irisin in KO male mice, with AAV8-GFP as the control, and placed them on the same low Ca diet. We chose male mice due to the highly significant effect on bone mass and strength we saw in the KO males compared to WT males on a low-calcium diet. The irisin injection rescued the skeletal phenotype in KO male mice, shown by the higher cortical bone area fraction and the lower endosteal perimeter (Fig 2G). There was a tendency for higher ultimate force and stiffness in the KO males that received the AAV8-irisin injection, however, this did not reach statistical significance (Fig 2H). These data show that the observed effects in the FNDC5 null animals are due to an absence of irisin.

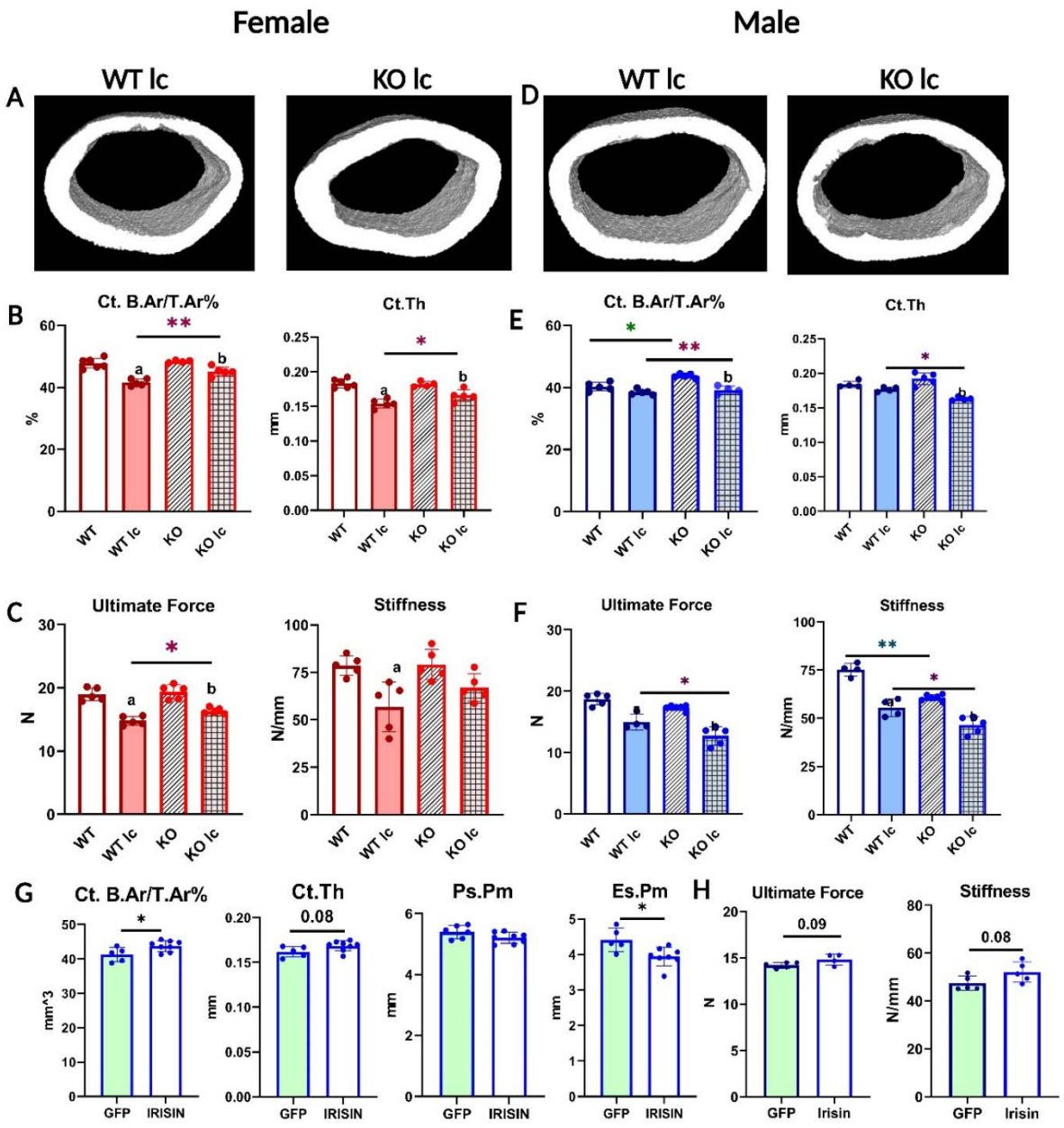

Fig 2: FNDC5 KO female and male mice have opposite responses to a low- calcium diet with regard to bone composition, structure, and mechanics, and irisin injection rescues FNDC5 KO male mice phenotype under a low-calcium diet

A: Representative µCT images of femoral midshaft cortical bones from WT low- calcium diet female mouse (WT lc) and KO low-calcium diet female mouse (KO lc).

B: Female femoral midshaft cortical bone parameters of WT control (WT), WT low-calcium diet (WT lc), KO control (KO), and KO low-calcium diet (KO lc) mice reported as cortical bone area fraction (Ct. B.Ar/T.Ar%) and cortical thickness (Ct.Th).

C: Mechanical properties of femurs from female WT and KO control and low- calcium diet reported as

ultimate force and stiffness.

D: Representative µCT images of femoral midshaft cortical bones from WT low-calcium diet male mice (WT lc) and KO low-calcium diet male mice (KO lc).

E: Male femoral midshaft cortical bone parameters of WT control (WT), WT low-calcium diet (WT lc), KO control (KO), and KO low-calcium diet (KO lc) mice reported as cortical bone area fraction (Ct. B.Ar/T.Ar%) and cortical thickness (Ct. Th).

F: Mechanical properties of femurs from male WT and KO control and low- calcium diet reported as ultimate force and stiffness.

n= 4-5/group. a= Significantly different from WT, b= Significantly different from KO, *= p< 0.05, **= p< 0.01. 2-way ANOVA was performed. As depicted here, red is female, and blue is male.

G: µCT measurement of femoral cortical bone of AAV8-GFP or AAV8-irisin injected male KO mice after a 2-week low calcium diet, reported as cortical bone area fraction (Ct. B.Ar/T.Ar%), cortical thickness (Ct. Th), periosteal parameter (Ps.Pm), and endosteal parameter (Es.Pm).

H. Mechanical properties of femurs from male KO low-calcium diet mice injected with AAV8-GFP or AAV8-irisin reported as ultimate force and stiffness.

n= 5-7/group, *= p< 0.05. Student's t-test was performed for statistical analysis between male KO GFP vs irisin-injected mice. As depicted here, green shaded bars represent GFP-injected mice.

Osteocytes from female and male KO mice respond differently to a low- calcium diet

To investigate if the bone loss was due to osteoclast or osteocyte activation, tibiae from all the groups were TRAP-stained. Under a normal control diet, the tibia from both KO female and male (Fig. 3A) mice had fewer TRAP-positive osteocytes compared to their WT counterparts. This indicates that their osteocytes were less 'primed' or 'activated' for resorption.

Under a low calcium diet, the number of TRAP-positive osteocytes increased in both WT and KO female mice, similar to lactation (Fig 3A, Table 1); however, the total number was still significantly lower in the KO females than the WT females. The low calcium diet increased TRAP-positive osteocytes in both WT and KO male mice. The KO male mice had a significantly higher level of increase (Fig 3A, Table 1), and had significantly higher TRAP-positive osteocytes compared to WT. This indicates an increased activation of osteocytes in the KO males and suggests higher osteocytic bone resorption.

There was no significant difference between WT and KO mice in osteoclast numbers per bone perimeter for both females and males (Fig. 3B). Both WT and KO females had an increase in their multinucleated TRAP-positive osteoclast number with a low-calcium diet, however, KO females had a significantly lower number of osteoclasts compared to WT females on a low-calcium-diet (Fig 3B). Similarly, under a normal diet, there was no difference in the number of osteo- clasts between male WT and KO. Under a low-calcium diet, osteoclast numbers increased in both groups, however, there was no

significant difference between WT and KO male mice (Fig. 3B). We also measured osteoblast numbers per bone perimeter. There was no difference in osteoblast numbers in either female or male normal or low-calcium diet mice groups (data not shown).

Under normal control diet conditions, female WT mice had significantly higher osteocyte lacunar area compared to WT males (Fig 3C, 3D). There was no significant difference between FNDC5 KO female and male mice with regards to osteocyte lacunar area. This indicates that under control conditions, female osteocytes have more resorptive activity. On a low calcium diet, all the groups have increased osteocyte lacunar area, indicating an increased level of osteocytic osteolysis (Fig 3E). However, in female KO mice, the average lacunar area is significantly less than in WT female mice, similar to what was observed with the lactation response. The male KO mice, on the other hand, have significantly larger lacunar areas compared to WT males on a low calcium diet, suggesting in- creased osteocytic osteolysis. Together these data show that bones from female KO mice are more resistant to calcium-demanding conditions, but the deletion of FNDC5/irisin from males makes them more susceptible to bone loss under calcium-demanding conditions. This also shows that male and female KO mice respond completely differently to the challenge of calcium deficiency.

Serum RANKL levels increased in all the low calcium diet groups compared to control diet groups (Fig 3F). There was no significant difference between WT and KO female mice and between WT and KO male mice. Serum PTH was measured because decreases in serum calcium stimulate the parathyroid gland to release PTH to remove calcium from bone to maintain normal calcium levels ***Jahn et al*** (***2017***); ***Matikainen et al*** (***2021***). PTH levels significantly increased in WT females and WT and KO males when subjected to a low calcium diet compared to the control diet (Fig 3G), however, the KO female group did not have a statistically significant increase in PTH levels. There was no significant difference in serum calcium levels in any of the groups (8-10 mg/dL range for all groups), which indicates that the elevated PTH is maintaining normal circulating calcium levels in these mice (Fig 3H).

Since FNDC5/irisin is robustly produced in skeletal muscle, we wanted to determine if the deletion of FNDC5/irisin affects muscle function, under either a normal or a low calcium diet. *In vivo* and *ex vivo* muscle contractility functions were performed in these mice. No difference was found between WT and KO mice on either a normal or a low calcium diet (Sup Fig 2). This indicates deletion of FNDC5 is not affecting muscle function and that bone resorption is releasing sufficient calcium into the circulation to maintain calcium homeostasis and supplying sufficient calcium for skeletal muscle function.

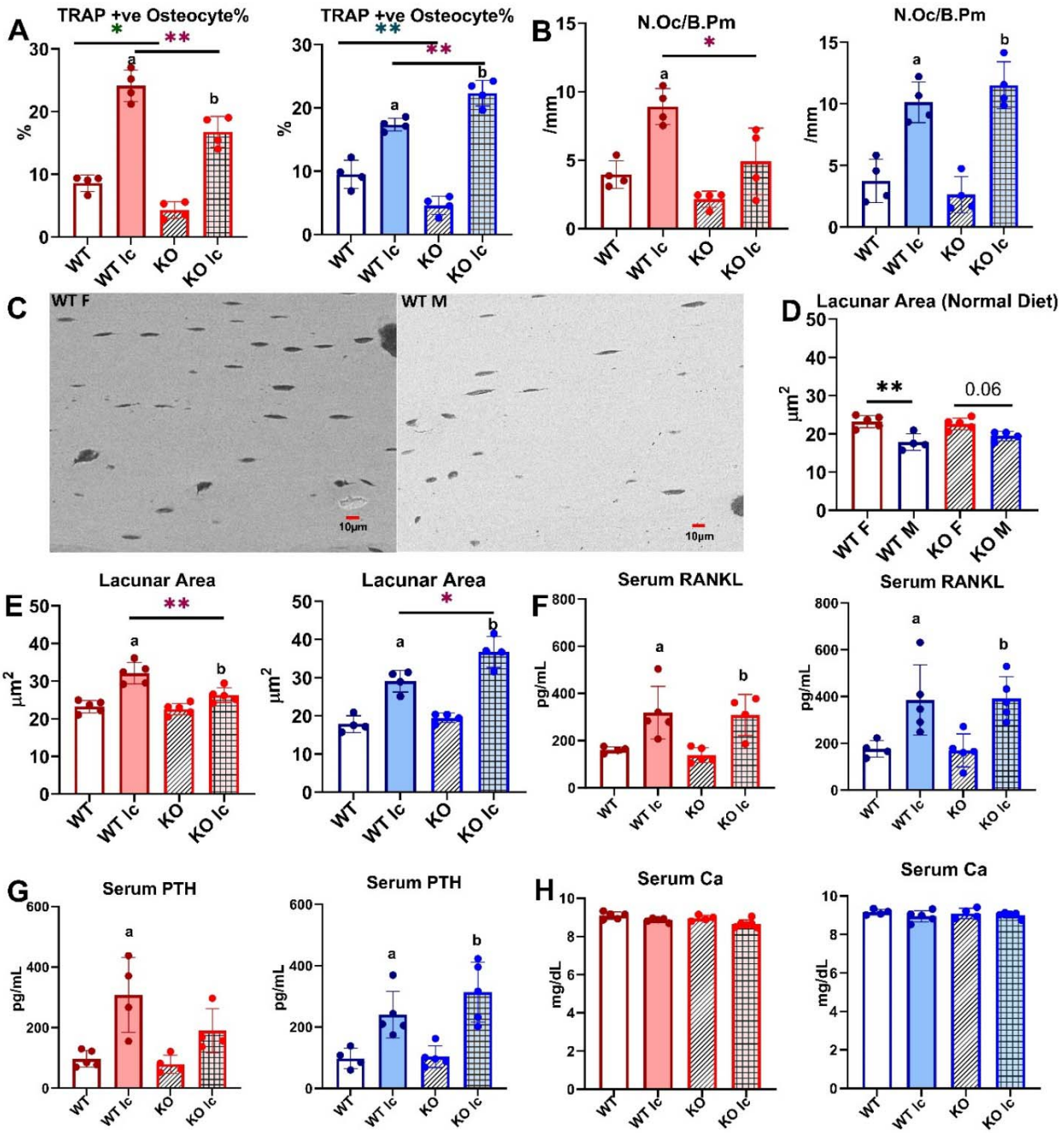

Fig 3: Osteocytes from female and male KO mice respond differently to a low-calcium diet

A: Percentage of TRAP-positive (+-ve) osteocytes in female and male WT and KO mice given a normal or a low-calcium diet.

B. Osteoclast number (N.Oc/B.Pm) in WT and KO female and male mice given a normal or a low-calcium diet.

C: Representative BSEM images depicting osteocyte lacunar area in femurs from WT female (WT F) and WT male (WT M) given a normal diet at 450X magnification.

D. Osteocyte lacunar area in WT and KO female and male mice given a normal diet.

E: Lacunar area in female and male WT and KO mice given a normal or a low- calcium diet.

F: Serum RANKL levels in female and male WT and KO mice given either a normal diet or a low-calcium diet.

G: Serum PTH levels in female and male WT and KO mice given either a normal diet or a low-calcium diet.

H: Serum calcium levels in female and male WT and KO mice given either a normal diet or a low-calcium diet.

n= 4-5/group. a= Significantly different from WT, b= Significantly different from KO, *= p< 0.05, **= p< 0.01. 2-way ANOVA was performed. As depicted here, red is female, and blue is male.

Table 1: Bone Parameters and Serum Markers		% Change in female		% Change in male	
	Change	WT	KO	WT	KO
Bone Area	Decrease	13%	7% *	2%	13% *
Bone Area Fraction	Decrease	17%	11% *	7%	23% *
Cortical Thickness	Decrease	19%	13% *	4%	15% *
Osteoclast Number/Bone Perimeter	Increase	125%	127%	170%	336% *
TRAP-positive Osteocytes	Increase	180%	290% *	85%	388% *
Osteocyte Lacunar Area	Increase	38%	16% *	60%	89% *
Serum PTH	Increase	150%	75% *	70%	164% *
Serum RANKL	Increase	100%	118%	119%	130%

Table 1: FNDC5 KO female and male mice have opposite responses to a low-calcium diet compared to WT female and male mice where female KO mice are protected but male KO mice have greater bone loss than WT.

Percentage changes in different bone and serum parameters of WT and KO female and male mice with a 2-week low-calcium diet. *= $p<0.05$ compared to WT.

Female and male osteocyte transcriptomes are distinctly different

Total RNA sequencing of osteocyte-enriched bone chips from female and male WT mice revealed significant sex-dependent differences in the osteocyte transcriptome under normal conditions (Fig. 4A, C, F). The major differentially expressed genes were involved in the steroid, fatty acid, cholesterol, lipid transport, and metabolic processes. Compared to male WT mice, female WT mice had an approximately 2-3-fold higher expression of very low-density lipoprotein receptor (*Vldlr*), voltage-dependent calcium channel T type alpha 1H subunit (*Cacna1h*), aldehyde dehydrogenase (*Aldh1l2*), and a 2-3-fold lower expression of apolipoproteins *Apoa1*, *Apoa2*, *Apoa4*, *Apoc3* and others involved in steroid and fatty acid metabolic process. There was also a 2-3-fold lower expression of several lipid and solute carrier genes and apolipoprotein genes in female WT compared to male WT. This suggests that male osteocytes may be greater regulators and utilizers of these sources of energy than female osteocytes.

Differences were also observed in genes involved in extracellular matrix organization pathways, bone development, ossification, bone remodeling, and re- sorption pathways. Female WT osteocytes have higher expression of genes shown to be highly expressed in osteocytes during lactation compared to male WT osteocytes. These include *Tnfsf11* (RANKL, 2.7-fold), *Ctsk* (2.5-fold), *Acp5* (TRAP, 2.2- fold), *Mmp13* (2.7-fold), osteoclast associated receptor (*Oscar*, 4.6-fold), macrophage stimulating 1 receptor (*Mst1r*, 3-fold), as well as several collagen genes and bone formation and mineralization genes including alkaline phosphatase (*Alpl*, 2.4-fold), periostin (*Postn*, 2.6-fold), and *Dmp1* (2.2-fold). *TGFβ3* was expressed higher in the WT females compared to WT males, but no significant difference was found in either *TGFβ1* or *TGFβ2* expression levels between WT females and males. This suggests that the higher expression of bone formation genes may be to accommodate the rapid replacement of the perilacunar matrix with weaning. The upregulated and downregulated pathways in WT females compared to WT males are depicted in Fig. 4.

Female and male KO osteocyte transcriptomes have fewer differences compared to WT female and male transcriptomes

KO female and KO male osteocyte transcriptomes significantly differed in pathways facilitating ossification and bone mineralization, and extracellular structure and matrix organization (Fig. 4B, F). In KO females, several collagen genes such as *Col2a1*, *Col5a2*, *Col8a2*, and *Col11a1* were 2-4-fold greater compared to KO males. Bone formation genes including *Alpl* (2.5-fold), osteocalcin

(*Bglap*, 2.7-fold), *Postn* (2.9-fold), and *Wnt4* (2.4-fold) were also more highly expressed in KO females compared to KO males, however, the resorption genes including *Acp5* and *Ctsk* were not significantly different between KO female and KO male osteocytes. *TGFβ3* was expressed higher in the KO females compared to KO males, similar to the WTs.

The transcriptomes of WT and KO male osteocytes differed significantly, with much lower expression of genes in pathways involving steroid, fatty acid, lipid, and cholesterol transport and metabolic processes in the KO males compared to WT males (Fig. 4C, F). A 2-4-fold downregulation of genes coding for solute carriers, aldehyde oxidase, and fatty acid binding proteins was observed in KO males, while *Oscar* and *Mst1r* are 2-3-fold higher in KO males compared to WT males. In contrast, a relatively small number of genes, 40, were differentially expressed between WT female and KO female osteocytes which reflects the lack of differences in bone morphology and bone mechanical properties (Fig. 4D, F).

Fig 4: Female and male wildtype osteocyte transcriptomes are distinctly different; however, female and male KO osteocyte transcriptomes have fewer differences compared to WT female and male transcriptomes.

A: Volcano plot showing the significantly regulated genes between WT female control (WT F) and WT male control (WT M) osteocyte transcriptome.

B: Volcano plot showing the significantly regulated genes between KO female control (KO F) and KO male control (KO M) osteocyte transcriptome.

C: Volcano plot showing the significantly regulated genes between WT male control (WT M) and KO male control (KO M) osteocyte transcriptome.

D: Volcano plot showing the significantly regulated genes between WT female control (WT F) and KO female control (KO F) osteocyte transcriptome.

E: Heat map showing the differentially expressed genes among WT female control (WT F), WT male control (WT M), KO female control (KO F), and KO male control (KO M) osteocyte transcriptome.

F: Gene set enrichment analysis of Gene Ontology (GO) analysis of the significantly regulated genes between WT female control (WT F) and WT male control (WT M) osteocyte transcriptome, between KO female control (KO F) and KO male control (KO M) osteocyte transcriptome, WT male control (WT M) and KO male control (KO M) osteocyte transcriptome, and WT female control (WT F) and KO female control (KO F) osteocyte transcriptome. The figure shows the union of the top 10 GO terms of each analysis. If a term in the union, besides the top 10, is also significant (adjusted p-value less than 0.05 was used for GO analysis) in an analysis, it is also included in the figure.

The latter group in the figure's title is the reference group. n=3/group. For DEG analys unadjusted p-value <0.01 was used.

With calcium deficiency, genes responsible for osteocytic osteolysis are lower in the female KO compared to the female WT osteocyte transcriptome

Calcium deficiency in WT female mice induced higher expression of osteoclast and resorption genes compared to WT females on a normal diet (Fig. 5A, E). *Acp5*, *Ctsk*, *Pth1r*, and *Mst1r* were elevated 2-4-fold in the calcium-deficient WT females. Real-time PCR analysis of osteocytes also showed an increase in *Tnsfs11*, *Acp5*, and *Ctsk gene* expression levels in the calcium-deficient WT females compared to WT females on a normal diet. There was no difference in *Sost* expression (Sup Fig 2D). Additionally, five different Mmps (*Mmp13*, *Mmp15*, *Mmp2*, *Mmp16*, and *Mmp14*) were upregulated 2-3.5-fold in the WT calcium-deficient females. These are genes thought to play a role in osteocytic osteolysis. Bone formation and remodeling genes including *Bglap*, *Bglap2*, *Alpl*, *Wnt 5a*, and *Wnt 2b* were upregulated 2-5-fold in the WT low calcium diet group compared to WT female normal diet group as well. These genes may be increased to provide quick bone formation upon return to normal calcium demand.

Calcium deficiency in KO female mice also induced increased expression of a number of osteoclast and resorption genes including *Ctsk* (2.8-fold), *Mmp13* (3- fold), and *Oscar* (2.6-fold) in comparison to KO female osteocytes on a normal diet (Fig. 5B, E). However, unlike the WT osteocytes, expression levels of *Acp5* and *Pth1r* were not different in osteocytes from KO female mice on a normal diet or a low calcium diet. Real-time PCR analysis also showed an increase in *Ctsk* gene expression level in the calcium-deficient KO females compared to KO females on a normal diet, with no significant difference in the expression levels of *Tnfsf11*, *Acp5*, and *Sost* genes (Sup fig 2D).

Next, we compared KO female mice on a low-calcium diet to WT female mice on a low-calcium diet (Fig. 5C, E). Several bone resorption genes were lower by 2-fold in KO females, including *Tnsfs11 and Mmp15*. Real-time PCR analysis also showed a significantly lower expression of the *Tnsfs11* gene in the calcium- deficient KO females compared to calcium-deficient WT females (Sup Fig 2D). Additionally, bone formation genes including *Alpl*, *Bglap*, *Wnt2b*, *Col1a1*, *Col1a2*, and *Postn* were also approximately 2-fold lower in the KO low calcium females compared to WT low calcium females. This suggests that female KO osteocytes are less responsive to calcium deficiency than female WT osteocytes.

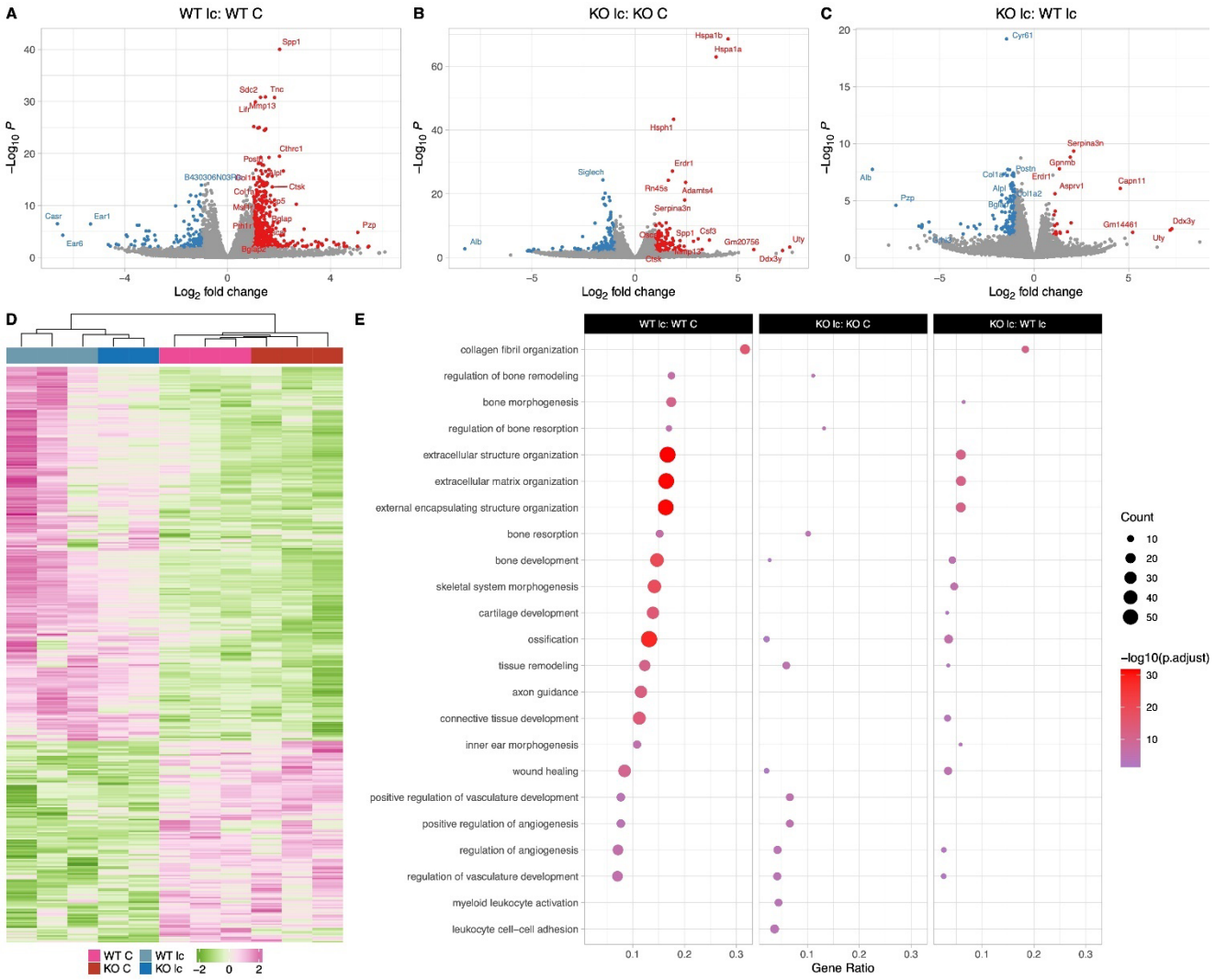

Fig 5: The Osteocyte transcriptomes from female WT and KO mice are distinct when challenged with a low-calcium diet

A: Volcano plot showing the significantly regulated genes between WT female control (WT C) and WT female low-calcium diet-fed mice (WT lc) osteocyte transcriptome.

B: Volcano plot showing the significantly regulated genes between KO female control (KO C) and KO female low-calcium diet-fed mice (KO lc) osteocyte transcriptome.

C: Volcano plot showing the significantly regulated genes between WT female low-calcium diet-fe mice (WT lc) and KO female low-calcium diet-fed mice (KO lc) osteocyte transcriptome.

D: Heat map showing the differentially expressed genes among WT female control (WT C), WT female low-calcium diet-fed mice (WT lc), KO female control (KO C), and KO female low-calcium diet-fed mice (KO lc) osteocyte transcriptome.

E: Gene set enrichment analysis of Gene Ontology (GO) analysis of the significantly regulated genes between WT female control (WT C) and WT female low-calcium diet-fed mice (WT lc) osteocyte transcriptome, between KO female control (KO C) and KO female low-calcium diet-fed

mice (KO lc) osteocyte transcriptome, and WT female low-calcium diet-fed mice (WT lc) and KO female low- calcium diet-fed mice (KO lc) osteocyte transcriptome. The figure shows the union of the top 10 GO terms of each analysis. If a term in the union, besides the top 10, is also significant (adjusted p-value less than 0.05 was used for GO analysis) in an analysis, it is also included in the figure.

The latter group in the figure's title is the reference group. n=2-3/group. For DEG analys unadjusted p-value <0.01 was used.

With calcium deficiency, genes responsible for bone resorption, bone formation, and lipid metabolism are differentially regulated in the osteocyte transcriptome in male KO mice compared to male WT mice

Calcium deficiency in WT male mice caused a 2-7-fold increased expression of *Tnsfs11*, *Acp5*, *Ctsk*, *Oscar*, and *Mst1r* in their osteocyte transcriptome compared to WT males on a normal diet (Fig. 6A, E). Real-time PCR validation also showed a similar increase in *Tnsfs11*, *Acp5*, and *Ctsk* gene expression levels in the calcium- deficient WT males compared to WT males on a normal diet (Sup Fig 2E). Bone formation and remodeling genes including *Postn*, *Col1a1*, *Col1a2*, *Bglap*, and *Wnt4* were also elevated 2-4-fold in the WT male low calcium diet compared to the WT normal diet control group.

Multiple genes involved in the steroid and fatty acid metabolic process pathways as well as lipid catabolic processes were downregulated 2-7-fold in the calcium-deficient WT males compared to WT males on a normal diet. These genes include several solute carrier family protein genes *Slc27a2* and *Slc27a5*, several apolipoprotein genes including *Apoa1*, *ApoB*, and *Apoc1*, several cyp genes including *Cyp2e1* and *Cyp7a1*, and *Plin1*.

Similarly, osteocytes from KO males on a low calcium diet had a 2-4-fold higher expression of osteoclast genes such as *Tnsfs11*, *Oscar*, and *Car3* and a 2-5-fold upregulation of bone formation genes such as *Col1a1*, *Col1a2*, *Alpl*, *Bglap*, and *Postn* compared to osteocytes from KO males on a normal diet (Fig. 6B, E). Therefore, genes responsible for bone resorption and bone formation were increased in both WT and KO with calcium deficiency. Real-time PCR data showed an increase in *Tnsfs11*, Acp5, and *Ctsk* gene expression levels in the calcium-deficient KO males compared to KO males on a normal diet, validating the RNA sequencing data (Sup Fig 2E).

When KO males were compared to WT males on a low calcium diet (Fig. 6C, E), there was a 2-3-fold higher expression of bone resorption genes including *Oscar* and *Mst1r* in the KO low calcium diet males compared to WTs. Several collagen formation genes and ossification genes including *Col3a1*, *Col8a2*, *Tnn*, *Aspn*, and *Igfbp6* were also significantly downregulated in the KO males on a low-calcium diet compared to WTs on a low-calcium diet. It is not clear whether these also play a role in the increased bone resorption observed with calcium deficiency in KO males. Real-time PCR analysis showed no significant difference in expression levels of *Tnsfs11*, *Acp5*, *Sost*, and *Ctsk* genes between calcium-deficient KO males and calcium-deficient WT males, reflecting the RNA sequencing data (Sup Fig 2E). No significant difference was observed in expression levels of genes involved in the lipid catabolic process

pathway or fatty acid metabolism pathways.

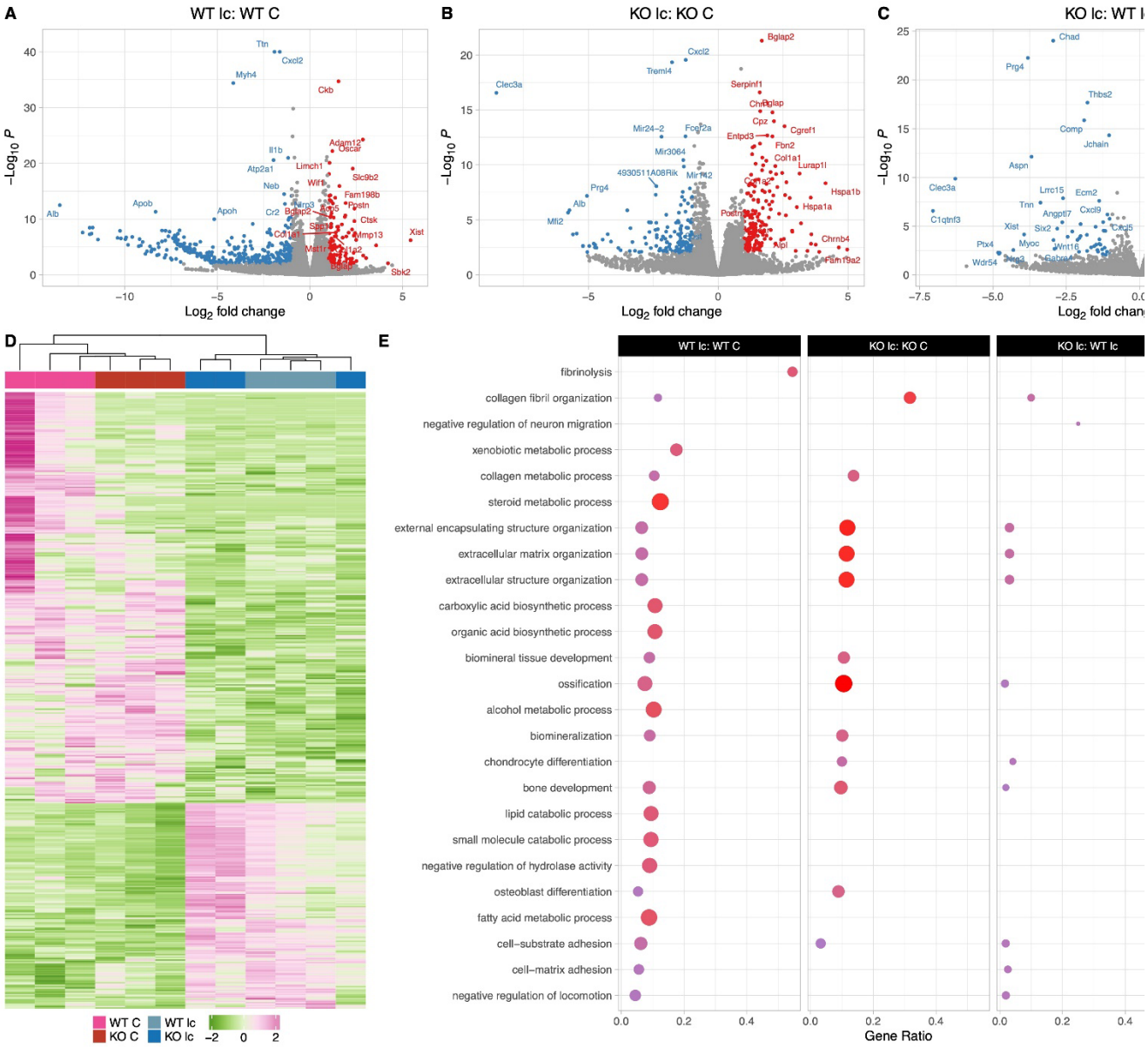

Fig 6: The Osteocyte transcriptomes from male WT and KO mice are dis- tinct when challenged with a low-calcium diet

A: Volcano plot showing the significantly regulated genes between WT male control (WT C) and WT male low-calcium diet-fed mice (WT lc) osteocyte transcriptome.

B: Volcano plot showing the significantly regulated genes between KO male control (KO C) and KO male low-calcium diet-fed mice (KO lc) osteocyte transcriptome.

C: Volcano plot showing the significantly regulated genes between WT male low-calcium diet-fed mice (WT lc) and KO male low-calcium diet-fed mice (KO lc) osteocyte transcriptome.

D: Heat map showing the differentially expressed genes among WT male control (WT C), WT male

low-calcium diet-fed mice (WT lc), KO female control (KO C), and KO male low-calcium diet-fed mice (KO lc) osteocyte transcriptome.

E: Gene set enrichment analysis of Gene Ontology (GO) analysis of the significantly regulated genes between WT male control (WT C) and WT male low- calcium diet-fed mice (WT lc) osteocyte transcriptome, between KO male control (KO C) and KO male low-calcium diet-fed mice (KO lc) osteocyte transcriptome, and WT male low-calcium diet-fed mice (WT lc) and KO male low-calcium diet-fed mice (KO lc) osteocyte transcriptome. The figure shows the union of the top 10 GO terms of each analysis. If a term in the union, besides the top 10, is also significant (adjusted p-value less than 0.05 was used for GO analysis) in an analysis, it is also included in the figure.

The latter group in the figure's title is the reference group. n=3/group. For DEG analys unadjusted p-value <0.01 was used.

Male and female osteocytes respond differently to calcium deficiency in a genotype-specific manner

In response to 2 weeks of calcium deficiency, WT female mice had higher expression of genes involved in extracellular matrix and structure organization as well as ossification compared to WT male mice with calcium deficiency. Calcium deficiency in WT female mice caused significantly increased expression of bone formation genes compared to WT males including several collagen genes such as *Col2a1*, *Col6a3*, *Col4a2*, as well as *Postn*, and *Bglap2*. This was accompanied by an increased expression of bone resorbing genes in WT females including several *Car* genes, *Mmp13*, *Mmp16*, *Tnsfs11*, and *Mst1r* in their osteocyte transcriptome compared to WT males on a low-calcium diet (Fig. 7A, C, D). This suggests that both bone formation and bone resorption are upregulated in WT females compared to WT males in response to calcium deficiency, and WT females undergo higher bone remodeling compared to WT males.

On the other hand, in response to calcium deficiency, KO female and male mice have less significantly differently expressed genes compared to WT females and males (Fig &B, C, D). The major upregulated bone formation genes in KO females compared to KO males include several collagen genes such as *Col2a1* and *Col8a2*. The major bone resorption gene that were upregulated in KO females compared to KO males were *Mmp13* and *Dcstamp*.

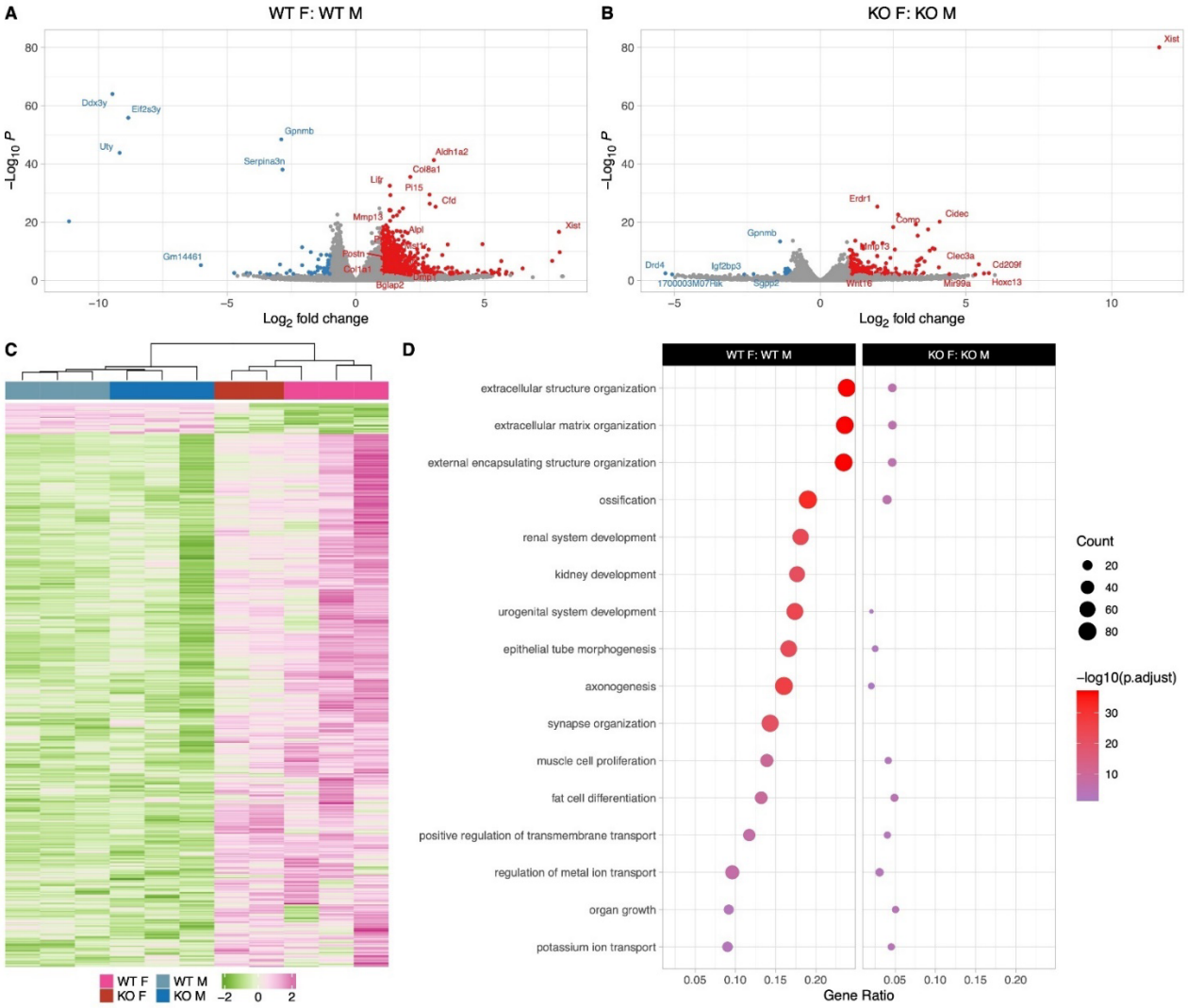

Fig 7: The Osteocyte transcriptomes from male and female mice are distinct when challenged with a low calcium diet

A: Volcano plot showing the significantly regulated genes between WT female low-calcium diet-fed (WT F) and WT male low-calcium diet-fed mice (WT M) osteocyte transcriptome.

B: Volcano plot showing the significantly regulated genes between KO female low-calcium diet-fed (KO F) and KO male low-calcium diet-fed mice (KO M) osteocyte transcriptome.

C: Heat map showing the differentially expressed genes among WT male low-calcium diet-fed mice (WT M), KO male low-calcium diet-fed mice (KO M), WT female low-calcium diet-fed (WT F), and KO female low-calcium diet-fed (KO F) osteocyte transcriptome.

D: Gene set enrichment analysis of Gene Ontology (GO) analysis of the significantly regulated genes between WT female low-calcium diet-fed (WT F) and WT male low-calcium diet-fed mice (WT M) osteocyte transcriptome, and between KO female low-calcium diet-fed (KO F) and KO male low-calcium diet-fed mice (KO M) osteocyte transcriptome. The figure shows the union of the top 10 GO terms of each analysis. If a term in the union, besides the top 10, is also significant (adjusted p-value less than

546 0.05 was used for GO analysis) in an analysis, it is also included in the figure.

547 The latter group in the figure's title is the reference group. n=2-3/group. For DEG analys

548 unadjusted p-value <0.01 was used.

Discussion

Irisin has been shown to be increased in the blood of humans and mice with exercise. Irisin, working mainly through its receptor αVβ5 integrin, has been shown to have powerful effects on fat, bone, and brain tissues ***Bostrom et al.*** (***2012***); ***Tsourdi et al.*** (***2022***); ***Korta et al.*** (***2019***); ***Islam et al.*** (***2021***); ***Kim et al.*** (***2018***); ***Colaianni et al.*** (***2017***); ***Wrann et al.*** (***2013***); ***Xin et al*** (***2016***); ***Wang et al.*** (***2017***); ***Bao et al.*** (***2022***); ***Zhang et al.*** (***2022***). With regard to bone, studies have generated complex and even contradictory results ***Erickson*** (***2013***); ***Maak et al.*** (***2021***); ***Colaianni and Grano*** (***2015***); ***Kim et al.*** (***2018***); ***Estell et al.*** (***2020***); ***Colaianni et al.*** (***2014***); ***Zhang et al.*** (***2018***). Of note, the majority of bone studies have been performed either exclusively on males, or females, but few on both. Most studies have used recombinant irisin treatment whereas we have focused on the effects of deleting irisin. Other studies have mainly examined the effects on osteoblasts and osteoclasts, whereas our studies have focused on osteocytes ***Kim et al.*** (***2018***).

Global deletion of FNDC5 on a normal diet had essentially no effect on bone in females, but in contrast, the null male mice have significantly more bone compared to wildtype males, but this bone has impaired mechanical properties. This suggests that the lack of FNDC5 is having no effect on the development or growth of the female skeleton, but does affect the male skeleton, increasing the size yet impairing matrix properties responsible for strength. Examination of their osteocytes showed that both female and male null mice have significantly fewer TRAP-positive osteocytes compared to their sex-matched wildtype controls suggesting that their osteocytes are more quiescent or less primed for bone resorption.

Challenging the null animals with calcium deficiency revealed dramatic differences in osteocytic osteolysis and osteoclast activation, two major functions of osteocytes. Deletion of FNDC5 in females is partially protective against calcium deficiency, but deletion in males accelerates both of these osteocyte functions resulting in greater bone loss compared to controls. We have shown previously that under calcium-demanding conditions such as lactation, osteocytes express genes previously thought only to be specific for osteoclasts including cathepsin K, TRAP, carbonic anhydrase, the proton pump V-ATPase, and others ***Qing et al.*** (***2012***) and shown that osteocytes are the major source of RANKL ***Nakashima et al.*** (***2011***); ***Xiong and O'Brien*** (***2012***); ***Xiong et al.*** (***2015***). In this study, lactating females lacking FNDC5 were partially resistant to bone loss, similar to ovariectomized females as previously published ***Kim et al.*** (***2018***). To determine the effects of calcium deficiency on males, mice were given a low-calcium diet for 2 weeks. Unlike the protective effects of FNDC5/irisin deletion in females, bone loss was exacerbated in null males compared to controls on a low calcium diet.

With two weeks of lactation and litter size comparable to wildtype controls, the null

583 female mice had less circulating RANKL, fewer TRAP-positive osteoclasts, fewer TRAP-positive
584 osteocytes, and smaller lacunar size. Our observation that the deletion of FNDC5/ irisin makes
585 lactating mice partially resistant to bone loss has an important implication with regard to the
586 purpose of lactation. Lactation is a critical period for pups as they obtain essential nutrients,
587 especially calcium, from the mother's milk for their proper growth. Calcium lost by the
588 mother's bone during lactation is rapidly replaced upon weaning with complete recovery of bone
589 mass within a week ***Qing et al.*** (***2012***); ***Wysolmerski*** (***2002***); ***Kalkwarf*** (***2004***); ***Kovacs*** (***2001***);
590 ***Wysolmerski*** (***2012***). Our data suggest that FNDC5/irisin acts as a regulator of calcium release from
591 maternal bones to fulfill the offspring demands during lactation. Therefore, irisin appears to play a
592 beneficial role in ensuring offspring survival and consequently, successful reproduction.

593 To determine if low calcium would have a similar effect on male FNDC5 null bone, both
594 males and females were subjected to a low-calcium diet for 2 weeks. The effects of a low-calcium
595 diet on female osteocytes and bone loss were essentially identical to the effects of lactation, with
596 two exceptions. First, serum RANKL levels were not significantly different between virgin and
597 lactating null females, while they were between null females on a normal compared to a calcium
598 diet suggesting that RANKL plays less of a role in lactation compared to calcium deficiency.
599 Secondly, the medullary cavity and endosteal bone in the low-calcium females were completely
600 protected in the FNDC5 null females but were not in the lactating FNDC5 null mice. Bone loss due to
601 lactation or due to dietary calcium deficiency may target different bone sites. Our unpublished
602 observations suggest that endosteal bone is removed faster than periosteal bone with lactation, but
603 this remains to be carefully validated. This difference may also be due to elevated PTHrP during
604 lactation ***Kovacs*** (***2001***), whereas hypocalcemia increases circulating PTH levels ***Goltzman*** (***2008***),
605 and it is not clear if hormones target distinct bone sites. Similar to the lactating FNDC5 null mice,
606 the null females placed on the low calcium diet had fewer TRAP-positive osteoclasts, fewer TRAP-
607 positive osteocytes, and smaller lacunar size. Serum RANKL levels increased in both wildtype and
608 null mice with dietary calcium deficiency, therefore, serum RANKL alone is not enough to explain
609 the partial protective effect of FNDC5 deletion against bone loss. In summary, female null mice
610 are not only resistant to bone loss due to estrogen deficiency as we showed previously ***Kim***
611 (***2018***) but are also resistant to calcium deficiency either due to an increase in PTHrP as with
612 lactation, or an increase in PTH as with a low calcium diet.

613 Osteoporosis manifests earlier in females due to menopause, but males also develop
614 osteoporosis but at an older age ***Johannesdottir et al.*** (***2013***); ***Johnston and Dagar*** (***2020***), and
615 the elderly are known to suffer from calcium deficiency which accelerates bone loss ***Kumssa et***
616 ***al.*** (***2015***); ***Body et al.*** (***2016***). Dietary calcium deficiency has been shown previously to affect
617 female and male bone differently where female rat bones are more sensitive to a low calcium diet

compared to males ***Geng and Wright*** (***2001***). Similarly, in our study, we saw that wildtype females were more affected by calcium deficiency and lost more bone compared to wildtype male mice. However, the opposite was observed for the FNDC5/irisin null mice, where female null mice were partially resistant, and male null mice were more susceptible to bone loss with calcium deficiency compared to their wildtype counterparts. Despite starting with more bone volume compared to wildtype, the FNDC5 null males had increased osteocyte lacunar area and lost more bone with dietary calcium deficiency compared to wild-type males. This greater bone loss can be explained through the dramatic increase of TRAP-positive osteocytes and TRAP-positive osteoclasts, but not by a significantly greater increase in circulating RANKL. This sex difference indicates that FNDC5/irisin may be involved in the regulation of calcium release from bone via osteocytes in a sex-dependent manner.

Lacunar area is an indicator of osteocyte regulation of their lacunar microenvironment. Here we report that osteocyte lacunar size is significantly larger in virgin wildtype female mice compared to same-age wildtype males. This difference in lacunar area indicates a distinction between female and male osteocyte function. The mammalian skeleton is a sexually dimorphic organ ***Sharma*** (***2023***), and female and male bones respond differently to circulating factors, hormones, and myokines as well as other challenges ***Kurapaty and Hsu*** (***2022***); ***Lu et al.*** (***2022***); ***Osipov et al.*** (***2022***). As osteocytes are regulators of bone formation and resorption ***Bonewald*** (***2011***); ***Dallas et al.*** (***2013***); ***Robling and Bonewald*** (***2020***), this sex difference may be due to differences in male and female osteocytes. A recent study by Youlten and colleagues has shown that male and female osteocyte transcriptomes are distinctly different ***Youlten et al.*** (***2021***). At 4 weeks of age, the female osteocyte transcriptome diverges from the male osteocyte transcriptome and these differences continue with age. A cluster of genes more highly expressed in female osteocytes compared to male osteocytes are those involved in bone resorption, the same ones elevated in osteocytes in response to lactation. These transcripts include genes necessary for osteocytic perilacunar remodeling and reduction in pH, which are essential for calcium removal ***Qing et al.*** (***2012***). This suggests that the larger lacunar area in female osteocytes compared to male osteocytes may be due to the higher expression of bone resorption genes.

The magnitude of the effect size due to FNDC5 deficiency appears modest with regards to the quantitative cortical bone parameters. However, if one examines the changes in osteocyte lacunar size and the mechanical properties of these bones, the differences are greater. As shown in Figure 3 E, the lacunar area of the wildtype females on a low calcium diet increases by over 30% and the FNDC5-null by less than 20%, while in the males it is approximately 38% in wildtype compared to 46% in null. According to Sims and Buenzli ***Buenzli***

653 ***and Sims*** (***2015***), a potential total loss of ~16,000 mm^3 (16 mL) of bone occurs through lactation
654 in the human skeleton. This was based on our measurements in lactation-induced murine
655 osteocytic osteolysis ***Qing et al.*** (***2012***). They used our 2D section of tibiae from lactating mice
656 showing an increase in lacunar size from 38 to 46 μm^2. In that paper we also showed that
657 canalicular width is increased with lactation. Therefore, this suggests dramatically lower
658 intracortical porosity due to the osteocyte lacunocanalicular system in female null mice
659 compared to female wild-type mice either with lactation or a low calcium diet and a dramatic
660 increase in intracortical porosity in null males compared to wild-type males on a low calcium
661 diet. Based on these data, using the FNDC5 null animals, we would speculate that the product
662 of FNDC5, irisin, is having a significant effect on the ultrastructure of bone in both males and
663 females challenged with a low calcium diet.

664 To begin to understand the molecular mechanisms responsible for the sex and genotype
665 differences, we compared the osteocyte transcriptomes of 5-month-old female and male, wildtype
666 and null mice. Our results show that the osteocyte transcriptomes of female and male wildtype
667 mice are significantly different under normal conditions. A surprising difference we observed
668 but not described in the Youlten paper ***Youlten et al.*** (***2021***) was that compared to wildtype
669 female osteocytes, wildtype male osteocytes have much higher expression of genes involved in
670 steroid, lipid, and cholesterol metabolism and transport pathways, lipid and solute carrier
671 genes, and apolipoprotein genes. This suggests that osteocyte metabolism and bioenergetics
672 are distinctly different between wildtype females and wildtype males. We hypothesize that the
673 differentially expressed genes in these bioenergetic and metabolic pathways modulate bone
674 mass and formation and may shed light on the sexual dimorphism of bones. As these
675 differentially regulated pathways were not previously reported by Youlten and colleagues
676 ***Youlten et al.*** (***2021***), this may be due to differences in strain, housing, diet, or microbiome.
677 Another explanation is the greater osteocyte purity in our study as we used a series of collagenase
678 digestions and EDTA chelation to remove any surface cells which was not performed in the
679 Youlten paper ***Youlten et al.*** (***2021***).

680 A second major difference between female and male wildtype osteocytes was the higher
681 expression of genes involved in collagen matrix formation, bone mineralization, remodeling,
682 resorption, and osteocytic osteolysis pathways in females compared to males. Many of the highly
683 expressed bone resorption genes in wildtype female osteocytes have been shown to be
684 elevated during lactation ***Qing et al.*** (***2012***) including *Acp5*, *Ctsk*, and *Mmp13*, all involved in
685 osteocytic osteolysis. This further supports our hypothesis that wildtype female osteocytes are
686 more primed for resorption compared to wildtype males, presumably to meet the increased
687 calcium demand during lactation, and correlates with the observed larger lacunae compared to

688 males.

689 TGFβ is another potential player in osteocyte perilacunar/canalicular remodeling.
690 Alliston and colleagues generated transgenic mice with reduced expression of the TGFβ Type II
691 receptor in mice expressing Dmp1-Cre ***Dole et al.*** (***2020***) (PMID: 32282961) and found a
692 significant difference in bone parameters and markers of osteocyte perilacunar remodeling
693 between the sexes. The females were subjected to lactation and the transgenics were found to
694 be resistant to osteocytic osteolysis compared to controls. However, these investigators did not
695 investigate the lacunar remodeling process in males as compared to females as was performed
696 in the present study using a low calcium diet. Their study does suggest that TGFβ is involved in
697 the osteocytic osteolysis that occurs with lactation, however, even though the transgenic males
698 showed a disrupted lacunocanlicular network compared to wildtype males, this does not
699 necessarily indicate a defect in perilacunar remodeling. It is more likely that the defect
700 occurred during bone formation when osteoblasts were differentiating into osteocytes. In our
701 study, we observed a higher expression of *TGFβ3* in wildtype female mice compared to
702 wildtype male mice, with no significant differences in *TGFβ1* or *TGFβ2* expression. This
703 suggests that *TGFβ3* may play a role in generating the larger lacunar area in wildtype females
704 compared to wildtype males through increased matrix related signaling.

705 Few differences were observed between wildtype female and null female osteocyte
706 transcriptomes as would be expected for bone morphometry and the only difference observed
707 was the number of TRAP-positive osteocytes. In contrast, osteocytes from wildtype males and
708 null males are significantly different with regards to fatty acid and lipid metabolism pathways
709 whereas null male mice have lower expression of these genes compared to wildtype males.
710 This suggests a role for irisin in lipid metabolism and bioenergetics in male osteocytes. Lower
711 expression in the null male mice may be responsible for the higher bone mass and inferior
712 biomechanical properties compared to wildtype males suggesting these pathways mediate the
713 effects of FNDC5/irisin on male bone.

714 Osteocytes from null females have higher expression of genes and pathways involved in
715 collagen matrix organization, ossification, and mineralization compared to null males. Unlike
716 wildtype males and females, there was no difference in expression of lipid, cholesterol, and fatty
717 acid metabolism genes in null males compared to null females. Again, this indicates that
718 FNDC5/irisin regulates male bone through these lipid-related pathways.

719 Lactation and calcium deficiency induce the same changes in females. Similar to that
720 reported previously for lactation ***Qing et al.*** (***2012***), osteocytes from wildtype female mice on a low
721 calcium diet exhibited an increase of several osteo- clast/resorption/lactation genes including *Acp5*,

Ctsk, *Oscar*, *Mst1r*, and *Pth1r* compared to wildtype females on a normal diet. Surprisingly, we also observed an increase in bone formation genes including *Col1a1*, *Alpl*, and *Bglap*. As osteocytic osteolysis is rapidly reversed within a week of weaning, the osteocyte may be preparing to rapidly reverse bone loss. We propose that once calcium is replenished, shutting off the proton pump will rapidly reverse the pH within the osteocyte lacunae, allowing bone-forming proteins such as alkaline phosphatase to become active to rapidly replace the osteocyte perilacunar matrix **Jahn et al.** (**2017**); **Andersson et al.** (**2003**); **Silver et al.** (**1988**); **Kaplan** (**1972**); **Farley and Baylink** (**1986**).

The main molecular mechanism responsible for the resistance of null female mice to calcium deficiency compared to wildtype female mice is lower expression of genes such as *Tnfsf11*, responsible for osteoclastic resorption. A correspondingly lower expression of bone formation genes including *Col1a1*, *Alpl*, and *Bglap* compared to wildtype females on a low-calcium diet was observed. The lower expression of both formation and resorption genes suggests a coupling of resorption with formation. Irisin appears to regulate calcium release in the female skeleton.

Osteocytes from wildtype male mice on a low calcium diet expressed higher levels of bone resorption genes including *Tnsfs11*, *Acp5*, *Ctsk*, *Oscar*, and *Mst1r* compared to wildtype male mice on a normal diet as expected. Like the females, there is a coupling with bone formation genes as there is also an increase in *Bglap* and *Col1a1*, suggesting the potential for osteocytes to rapidly replace their perilacunar matrix with calcium repletion. Similarly, the male null mice with calcium deficiency showed an increase in bone resorption genes including *Tnsfs11*, *Oscar*, and *Car3*, as well as an increase in bone formation genes such as *Alpl* and *Bglap* compared to null mice on a normal diet. The major differences between wildtype male mice with calcium deficiency and FNDC5-null male mice with calcium deficiency were the lower expression of genes involved in the extracellular matrix organization, ossification, and bone development pathways in the null male mice compared to wildtype males. This suggests a mechanism for how null male mice lose more bone with calcium deficiency compared to wildtype males.

Irisin could be having direct or indirect effects on osteocytes. Irisin can modulate adipose tissue **Bostrom et al.** (**2012**); **Zhang et al.** (**2014**); **Celi and Brown** (**2017**); **Luo et al.** (**2022**), can potentially modulate osteogenic differentiation of bone marrow mesenchymal stem cells through $\alpha V\beta 5$ **Zhu et al.** (**2023**) and bone marrow adipose tissue can modulate bone properties **Yeung et al.** (**2005**); **Rosen and Bouxsein** (**2006**); **Muruganandan and Sinal** (**2014**); **Styner et al.** (**2015**); **Schwartz et al.** (**2015**); **During** (**2020**) as well as osteocyte number and activity **Saedi A et al.** (**2019**, 2020). Irisin can modulate brain activity and signaling **Islam et al.** (**2021**); **Wrann et al.** (**2013**); **Young et al.** (**2019**); **Jo and Song** (**2021**); **Qi et al** (**2022**) through BDNF **Wrann et al.** (**2013**) and BDNF promotes osteogenesis in human bone mesenchymal stem cells **Liu et al.** (**2018**). Our data

do not show significant expression of *Fndc5* in osteocytes. Studies from our group have found no expression of *Fndc5* in primary osteoblasts and primary osteocytes (transcriptome analysis with a raw count of 8-12), however both skeletal muscle (gastrocnemius) and C2C12 myotubes have high expression of *Fndc5* (transcriptome raw count of 512-1000, unpublished). As such, we postulate that the effect of irisin on osteocytes is not an autocrine effect, but rather due to irisin production by skeletal muscle.

Irisin must bind to αVβ5 integrins to function. Osteocytes express high levels of this receptor which was first discovered using the female MLO-Y4 osteocyte-like cell line **Kim et al.** (**2018**). Integrins are usually stable in the cell membrane with a half-life of 12-24 hours **Moreno-Layseca et al.** (**2019**). In our RNA sequencing data, we observed a stable expression of both *ITGAV* and *ITGB5*, encoding integrins αV and β5 respectively, with no differences between either wildtype or null, male or female, calcium replete or calcium deficient mice. Recently it has been published that Hsp90α is necessary to facilitate irisin-αVβ5 binding **Mu et al.** (**2023**). *Hsp90a*, the gene encoding this heat shock protein, is very highly expressed in both wildtype and null male and female mice, with no significant regulation by diet. The high expression of Hsp90α in osteocytes may explain their significant and rapid responses to irisin **Kim et al** (**2018**).

In summary, during normal development and on a regular diet, FNDC5/irisin deletion has few if any effects on the female skeleton but a significant effect on the male skeleton resulting in more but weaker bone. However, with challenges, such as calcium deficiency, dramatic differences were observed. Our data suggest that irisin activates the osteocyte in females to initiate the removal of their perilacunar matrix and for bone resorption through osteoclast activation, presumably to provide calcium for reproduction purposes. In contrast, in males, irisin protects against osteocytic osteolysis and osteoclastic bone resorption under calcium-demanding conditions. This sex-specific effect may be due to the sexual dimorphism of the osteocyte transcriptome. We have discovered a new novel function of irisin to ensure the survival of offspring and that irisin is essential for male but not female skeletal development. These findings could have implications for understanding sex-dependent differences in bone diseases, such as osteoporosis, and lead to the development of sex- targeted therapies.

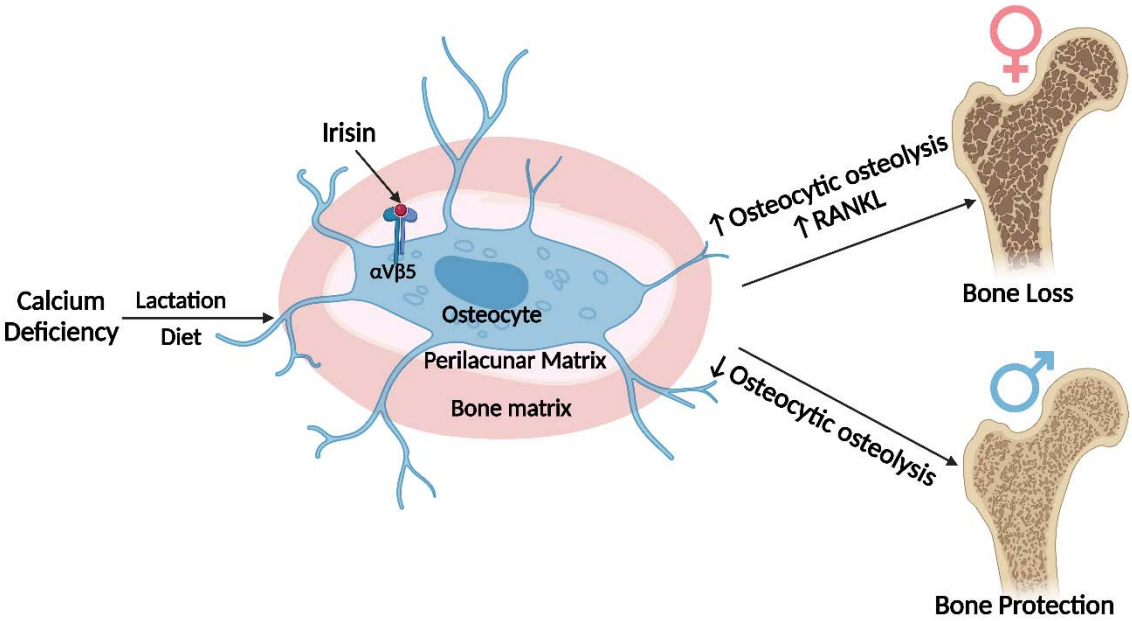

Fig 8: Graphical abstract (image was created using BioRender.com)

- No differences are observed in bone from Fndc5 /irisin null female, whereas null mal skeletons are larger but weaker compared to wildtype controls.
- With calcium deficiency, lactating female null mice are protected from bone loss due to osteocytic osteolysis, whereas male null mice on a low calcium diet lose greater amounts of bone compared to their wildtype controls.
- The osteocyte transcriptomes show wildtype males have higher expression of the steroid, lipid and fatty acid pathways which are lower in the null males, whereas the wildtype females have higher expression of genes regulating osteocytic osteolysis than null females.
- With calcium deficiency, female null osteocytes have lower while male null osteocytes have higher expression of osteocytic osteolysis genes compared to wildtype controls.

Methods

Animal Experiments

All animal experiments were performed per procedures approved by the Institutional Animal Care and Use Committee (IACUC) of the Indiana University School of Medicine. Heterozygous C57Bl/6J FNDC5 Knockout (KO) mice were provided by Dr. Bruce Spiegelman at Harvard University and bred in our facility to obtain homozygous global FNDC5 KO and wildtype (WT) control mice. Genotype was determined using a PCR reaction with primers targeting portions of exon 3 absent in KO (WT Forward: GCG GCT CGA GAG ATG AAG AA, WT Reverse: CAG CCC ACA ACA AGA AGT GC, KO Forward: GGA CTT CAA GTC CAA GGT CA, KO Reverse: CCT AAG CCC ACC CAA ATT AC). Mice were housed in a temperature-controlled (20–22°C) room on a 12-hour light/dark cycle with ad libitum food and water. Qualified veterinary staff and/or animal care technicians performed regular health check inspections.

For the lactation experiments, 4-month-old WT and FNDC5 global KO female mice were bred, delivered pups, and lactated for 2 weeks before sacrifice. Virgin WT and KO mice were used as controls. All animals were 4-5 months old at the time of sacrifice and analysis. For all lactating mice, the litter size ranged from 8-11 pups *Qing et al.* (*2012*).

For the low calcium diet experiments, 4-5-month-old male and female WT and FNDC5 global KO mice were fed either a control diet (0.6% calcium, Teklad, TD.97191) or a low calcium (Ca) diet (0.01% calcium, 0.4% phosphorus, Teklad TD.95027) for 2 weeks. Food was replaced every two days. Distilled water was used in place of tap water to control calcium intake. On the day of sacrifice, blood was collected under anesthesia, and mice were euthanized for sample collection, processing, and analysis *Qing* (*2012*); *Jahn et al.* (*2017*).

AAV8 injection

AAV8-irisin and AAV8–GFP constructs were obtained from Dr. Bruce Spiegelman at Harvard University. AAV8 Mouse ORF 1-140 (containing the N-terminal signal peptide and irisin) plus a five-amino-acid linker plus a C-terminal flag tag was cloned into the pENN.AAV.CB7.CI.pm20d1flag.WPRE.rBG vector (Addgene plasmid no. 132682). AAV8-GFP (pENN.AAV.CB7.CI.eGFP.WPRE.rBG), used as control, was obtained from Addgene (105542), and packaged at the UPenn Vector Core to a titer of 2.10 × 1013 GC per ml39. FNDC5 KO male mice were placed under anesthesia and injected into the tail vein with either AAV8-irisin or AAV8-GFP control (1 X 10^{10} GC per mouse) in 100 μL in PBS *Islam et al.* (*2021*). One week after injection with either the control virus containing GFP or the virus coding for circulating irisin, the mice were placed on a low-calcium diet for two weeks before sacrifice.

In vivo and *ex vivo* muscle contractility and electrophysiology measurement

In vivo plantarflexion torque was assessed one day before sacrifice (Scientific Inc, Canada) as described in *Pin et al.* (*2022*). Briefly, the mouse was placed under anesthesia and the left hind foot was

affixed to the force transducer aligned with the tibia at 90°. The tibial nerve was stimulated using monopolar electrodes (Natus Neurology, Middleton, WI). Maximum twitch torque was established by using a 0.2 ms square wave pulse. Peak plantarflexion torque was measured by using a stimulation of 0.2 ms delivered at 100Hz stimulation frequency.

In vivo electrophysiological functions were assessed one day before sacrifice with the Sierra Summit 3–12 Channel EMG (Cadwell Laboratories Incorporated, Kennewick, WA, USA) as described in ***Huot et al.*** (***2022***). Briefly, peak-to-peak and baseline-to-peak compound muscle action potentials (CMAP) were measured using supramaximal stimulations of <10 mA continuous current for 0.1 ms duration, and peak-to-peak single motor unit (SMUP) potentials were measured using an incremental stimulation technique. Motor unit number estimation (MUNE) was measured using the equation: MUNE = CMAP amplitude/average SMUP.

Ex vivo muscle contractility was measured in the extensor digitorum longus (EDL) muscle as described in ***Huot et al.*** (***2021***). EDL was collected from the mouse and mounted between a force transducer, and then submerged in a stimulation bath. The muscles were forced to contract, and data were collected using Dynamic Muscle Control/Data Acquisition (DMC) and Dynamic Muscle Control Data Analysis (DMA) programs (Aurora Scientific). The EDLs were weighed for normalization purposes.

Body composition assessment by dual-energy X-ray absorptiometry (DXA)

The right femurs from mice were dissected and cleaned of soft tissue, fixed in 4% paraformaldehyde (PFA) for 48 hours, and then transferred to 70% ethanol. Ex vivo DXA measurements were obtained using a faxitron (Faxitron X-ray Corp, Wheeling, IL) to measure bone mineral density (BMD) and bone mineral content (BMC) ***Essex et al.*** (***2022***).

Bone morphometry analysis by micro-computed tomography (μCT)

Right femurs were analyzed using a Skyscan 1176 μCT as described previously ***Pin et al.*** (***2022***). Briefly, specimens were scanned at 55 kV, 145 μA, high resolution, 10.5 mm voxel, and 200 ms integration time. For cortical parameters, three- dimensional images from a 1mm region of interest (ROI) of the mid-diaphysis were used to calculate total cortical bone area fraction (Ct. B. Ar/T. Ar%), cortical bone thickness (Ct. Th), marrow cavity area, periosteal perimeter (Ps. Pm), and endosteal perimeter (Es. Pm) according to ASBMR guidelines ***Bouxsein et al.*** (***2010***). For trabecular parameters, three-dimensional images reconstructed within the range of 0.5 mm from the most proximal metaphysis of tibiae were analyzed. Trabecular morphometry was performed by excluding the cortical bone from the endocortical borders using hand-drawn contours followed by thresholding and characterized by bone volume fraction (BV/TV), trabecular number (Tb. N), trabecular thickness (Tb. Th), trabecular spacing (Tb. Sp), and connectivity density (Conn.D) ***Kitase et al.*** (***2018***).

Tartrate-resistant acid phosphatase (TRAP) staining

Tibiae were stripped of soft tissue, fixed in 4% PFA for 48 hours, decalcified in 10% EDTA for 3-4 weeks, and processed into paraffin as described previously followed by sectioning (5 μm) and staining for TRAP activity using the standard naphthol AS-BI phosphate post coupling method and counterstained with toluidine blue ***Pin et al.*** (***2021***). Briefly, after equilibration in 0.2 M sodium acetate, 50 mM sodium tartrate, pH 5.0, for 20 min at RT, sections were incubated at 37°C in the same buffer containing 0.5 mg/ml naphthol AS-MX phosphate (Sigma Chem. Co., St. Louis, MO) and 1.1 mg/ml Fast Red Violet LB salt (Sigma) and counter- stained in toluidine blue. Images were taken at 5X and 40X using an Olympus BX51 fluorescent microscope and Olympus cellSense Entry 1.2(Build 7533) imaging software. TRAP-positive osteocytes and osteoclasts 1.5 mm distal from the growth plate were quantified using Osteomeasure software (OsteoMetrics.Inc) in a blind fashion. Toluidine blue-stained osteoblasts from the same sections were quantified 1.5 mm distal from the growth plate using the same software.

Osteocyte lacunar area measurement by Backscatter Scanning Electron Microscopy (BSEM)

Femurs were stripped of soft tissue and fixed in 4% PFA for 48 hours before proceeding to dehydration and embedding steps as previously described ***Qing et al.*** (***2012***). Briefly, femurs were dehydrated in graded ethanol and placed into acetone. Subsequently, the femurs were immersed in infiltration solution made of 85% destabilized methyl methacrylate (MMA, Sigma), 15% dibutyl phthalate (Sigma), 1% PEG400 (Sigma), and 0.7% benzoyl peroxide (Polysciences, Inc., Warrington, PA)/acetone until infiltration was complete. The femurs were then placed on pre-polymerized base layers, covered with freshly catalyzed MMA embedding solution (for 100 mL, 85mL MMA, 14mL dibutyl phthalate, 1mL PEG400, 0.33uL DMT, and 0.8g BPO), and incubated under vacuum until the MMA was polymerized. The polymerized blocks were trimmed, sequentially polished to a completely smooth surface, and coated with gold using a sputter coater (Desk V, Denton Vacuum, NJ, USA). Then BSEM (JEOL: JSM-7800F) was performed to image the osteocyte lacunae on the sectioned bone surface at 450X magnification starting 2 mm distal from the growth plate. Six fields from the endosteal and periosteal sides of the cortical bone were taken as described previously ***Qing and Bonewald*** (***2009***). Using ImageJ (NIH), the images were thresholded for background removal, binarized, and the lacunar area from each sample quantitated.

Mechanical testing using 3-point bending

Mechanical testing was performed essentially as described in ***Melville et al.*** (***2015***). Briefly, the left femurs were stripped of soft tissue, wrapped in PBS- soaked gauze, and stored at -20°C until use. Frozen femurs were brought to room temperature and mounted across the lower supports (8 mm span) of a 3- point bending platen on a TestResources R100 small force testing machine. The samples were tested in monotonic bending to failure using a crosshead speed of 0.05 mm/s.

Parameters related to whole bone strength were measured from force/displacement curves.

Serum RANKL analysis

The levels of RANKL were measured in mouse centrifuged serum by using an ELISA kit (Bio-Techne Corporation, Minneapolis, MN), according to the manufacturer's protocol.

Serum parathyroid hormone (PTH) analysis

Serum was obtained from terminal cardiac puncture and serum PTH levels were determined using the MicroVue Bone Mouse PTH 1-84 ELISA assay (Quidel Corp., San Diego, CA) according to the manufacturer's protocol.

Calcium measurement

Plasma calcium levels were determined using the Pointe Scientific calcium Reagent kit (Manufacturer and city). Briefly, diluted serum (1:4 in dH2O) was incubated with a working calcium color reagent for 1 min and the absorbance read at 575 nm using a spectrophotometer (BioTek Synergy HTX).

Sample collection and processing for RNA sequencing

Bulk RNA sequencing was performed on osteocytes from the control and low calcium diet, male and female, WT and KO mice. Osteocyte RNA was extracted from tibia and femur diaphyses after sequential digestion to remove surface cells including osteoclasts, osteoblasts, and lining cells as previously described ***Qing et al.*** (***2012***); ***Pin et al.*** (***2022***). Briefly, soft tissue was removed from the bones, the epiphyses were cut off and bone marrow was removed by flushing with PBS. The remaining midshafts were incubated at 37°C with 0.2% type 1 collagenase (Sigma) for 30 minutes, followed by chelation/ digestion in 0.53 mM EDTA/ 0.05% trypsin (Cellgro, Mediatech, Inc, Manassas, VA) at 37°C for 30 min followed by a second collagenase digestion. After each step, the bone chips were rinsed with PBS and after the final step, flash-frozen in liquid nitrogen, and pulverized in liquid nitrogen, with Trizol reagent (Qiagen, Carlsbad, CA) added to the resulting bone powder. Total RNA was isolated with an RNA purification kit (Qiagen miRNeasy mini kit) and DNase treatment to remove DNA contamination.

Library preparation and RNA sequencing

Total RNA samples were first evaluated for their quantity and quality using Agilent TapeStation. All the samples used for the sequencing had a RIN of at least 5. 100 nanograms of total RNA were used for library preparation with the KAPA total RNA Hyperprep Kit (KK8581) (Roche). Each resulting uniquely dual-indexed library was quantified and quality accessed by Qubit and Agilent TapeStation. Multiple libraries were pooled in equal molarity. The pooled libraries were sequenced on an Illumina NovaSeq 6000 sequencer with the v1.5 reagent kit. 100 bp paired-end reads were generated.

RNA-seq data analysis

The sequencing reads were first quality-checked using FastQC (v0.11.5, Babraham Bioinformatics, Cambridge, UK) for quality control. The sequence data were then mapped to the mouse reference genome mm10 using the RNA-seq aligner STAR (v2.7.10a) *Dobin et al.* (*2013*) with the following parameter: "--outSAMmapqUnique60". To evaluate the quality of the RNA-seq data, the number of reads that fell into different annotated regions (exonic, intronic, splicing junction, intergenic, promoter, UTR, etc.) of the reference genome was assessed using bamutils *Breese and Liu* (*2013*). Uniquely mapped reads were used to quantify the gene level ex- pression employing featureCounts (subread v2.0.3) *Liao et al.* (*2014*) with the following parameters: "-s 2 -Q 10".

Quality control of samples

During data quality control, one of the KO female control samples (sample 23) was found to have a similar proportion of reads on chromosome Y as in male mice and a very low expression of the gene Xist, typically highly expressed in females (Supplementary Figure 3A, 3B), therefore this sample was excluded from the analysis.

The WT female low-calcium diet samples (samples 16, 17, and 18) had low mapping percentages of 37%, 32%, and 61%, respectively. This may be due to bacterial contamination. The two possible methods to process these data are to filter all the possible contaminated reads before alignment or align the reads without filtering. However, filtering the possible contaminated reads before alignment may result in removing some reads from the mouse genome which is similar to the bacterial genome (causing lower gene expression). In contrast, using data without filtering may result in some genes having higher expression levels due to reads from the bacterial genome which are aligned to mice genes. We decided to perform a principal component analysis (PCA) using data without filtering and found that the samples clearly clustered into four groups: control male mice, control female mice, low-calcium diet male mice, and low-calcium diet female mice (Supplementary Figure 3C). Within each group, the separation of WT and KO mice is also clear. Due to contamination, samples 16 and 18 were slightly far apart from the others. However, contamination should not have a large global influence on the data as samples 16, 17, and 18 are close to the non-contaminated samples 5 and 6, also in the low-calcium diet female group. Additionally, we validated the data using qPCR with selected genes.

Differentially expressed gene analysis

The read counts matrix was imported to R *Team* (*2022*) and analyzed with DEseq2 *Love et al.* (*2014*). Within DESeq2, read counts data were normalized with median of ratios, and differentially expressed genes (DEGs) were detected after independent filtering. In DEG analysis, we first detected DEGs between different groups. Significant genes were defined as genes with an unadjusted p-value less

than 0.01 and absolute log2 fold change larger than 1. Gene set enrichment analysis was applied on gene sets from *Gene ontology resource: enriching a GOld mine* (*2021*) using R package clusterProfiler *Wu* (*2021*). p value of less than 0.05 was considered as significant for the gene ontology analysis. Several RNA sequencing and pathway figures were prepared with R packages ggplot2 *Wickham* (*2016*) and ComplexHeatmap *Gu* (*2022*). The data was deposited in NCBI GEO database (accession number GSE242445).

Real-time quantitative polymerase chain reaction (qPCR)

Total RNA was reverse transcribed to cDNA using the Verso cDNA Kit (Thermo Fisher Scientific). Transcript levels were measured by real-time PCR (Light Cycler 96; Roche), taking advantage of the TaqMan and SYBR Gene Expression Assay System (Thermo Fisher Scientific). Expression levels for RANKL (*Tnfsf11*, Forward primer: CCG AGC TGG TGA AGA AAT TAG, Reverse: CCC AAA GTA CGT CGC ATC

TTG), Cathepsin K (*Ctsk*, Primer Bank ID: Mm.PT.58.9655974, IDT), TRAP (*Acp5*, Mm.PT.58.5755766, IDT), and sclerostin (*Sost*, Mm00470479_m1, Applied Biosystems) were quantitated. Gene expression was normalized to β-2-microglobulin (*B2m*, Forward: ACA GTT CCA CCC GCC TCA CAT T, Reverse: TAG AAA GAC C A G TCC TTG CTG AAG) levels using the standard 2−ΔΔCt method.

Statistical Analysis

Data are expressed as individual data points. The statistical analysis was done by Prism 8.2 (GraphPad Software, San Diego, CA, USA) and R 4.3.0. When comparing three or more groups with two variables, a two-way analysis of variance (ANOVA) was used. To compare between two groups, the unpaired, two-tailed Student's t-test was used. Differences were considered significant at * $p < 0.05$, ** $p < 0.01$, and *** $p < 0.001$.

ACKNOWLEDGEMENTS:

We would like to thank the Center for Medical Genomics, the Small Animal Phenotypic Core, and the Histology and Histomorphometry Core at the Indiana Center for Musculoskeletal Health for help and advice with histological sample preparation. We would like to thank Dr. Yukiko Kitase, Dr. Eijiro Sakamoto, and Carrie Zhao for their help and advice with the experiments. This work was supported by NIH awards P01 AG039355 (to L.F.B).

Disclosures

The authors declare that they have no conflicts of interest.

Data Availability Statement

All data that support the findings of this study are available from the corresponding author upon reasonable request.

The osteocyte transcriptome data has been deposited into the NCBI GEO database. The accession number for the data is GSE242445.

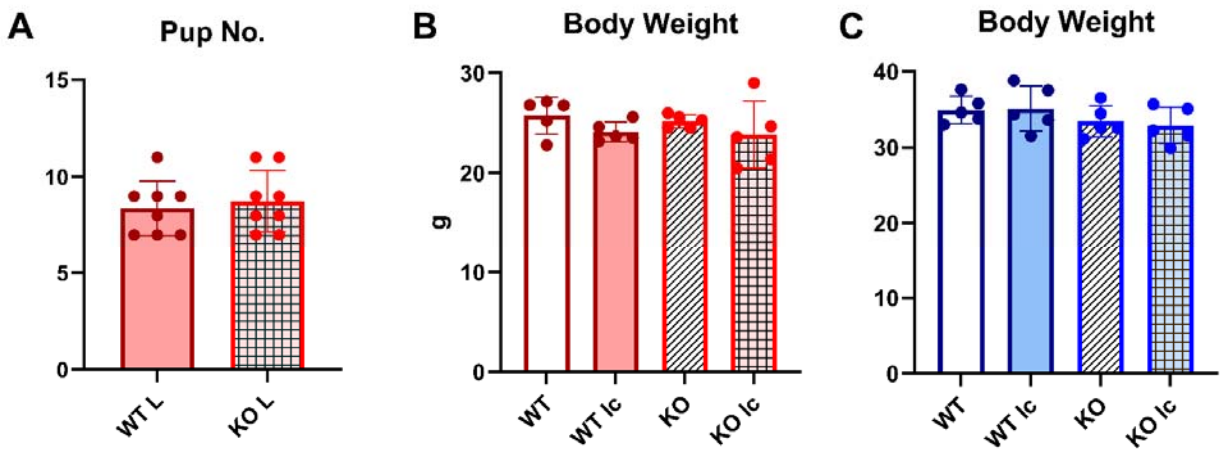

Supplementary Figure 1: Pup numbers for the lactation experiment, and body weight measurements for the lo calcium-diet experiment

Panel **A** shows total pup numbers in WT and KO female mice that underwent pregnancy and 2 weeks of lactation. There are no significant differences in the pup numbers between genotypes. Students t-test was performed for statistical analysis. n= 8/group.

panels **B** and **C** show total body weight of WT and KO female (B) and male (C) mice. No statistically significant difference was found among the groups, regardless of genotype or diet. 2-way ANOVA with Tukey's post hoc test was done. n= 4-5/group. As depicted here, red is female, and blue is male.

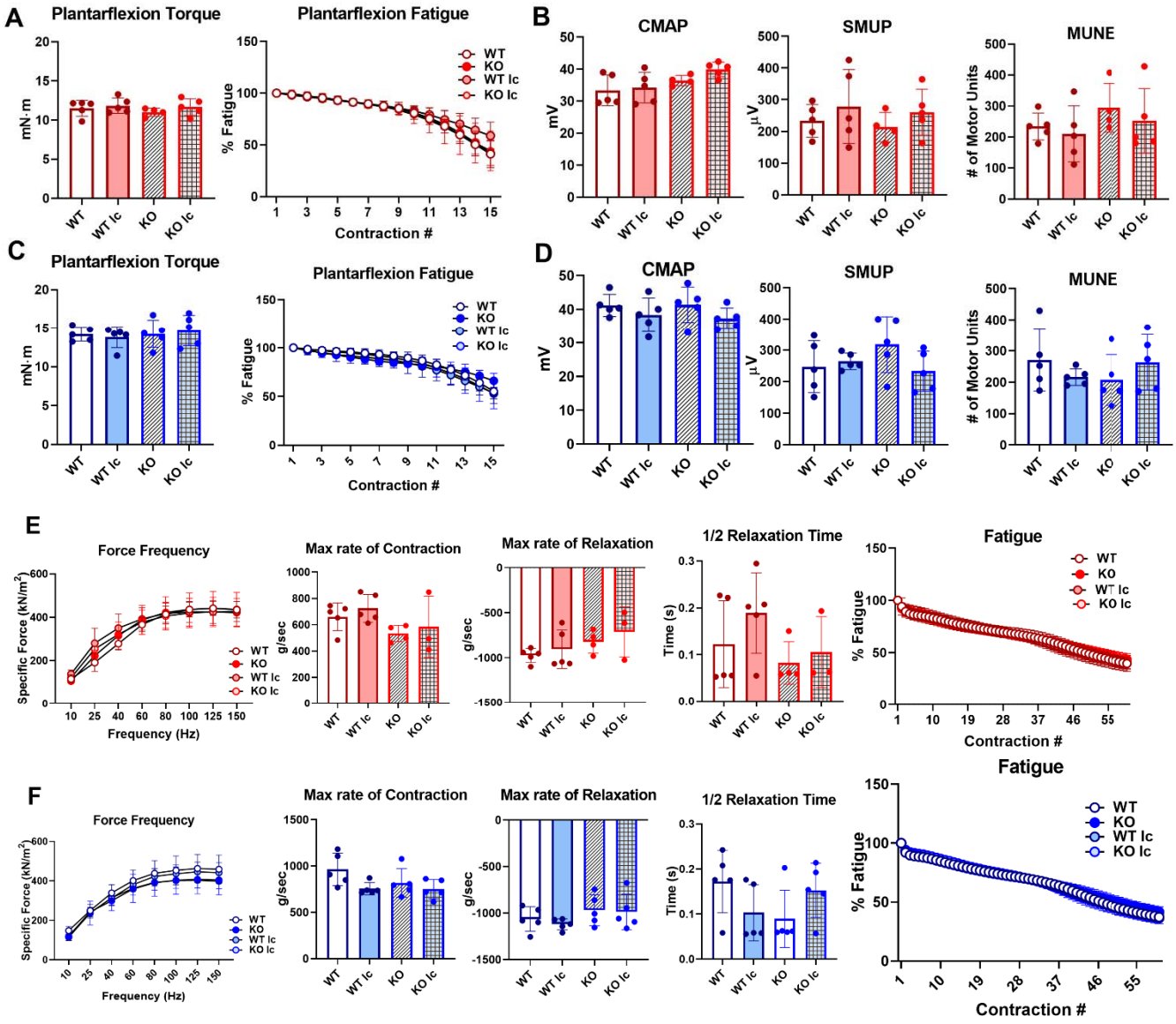

Supplementary Figure 2: Neither genotype nor dietary calcium alters muscle functions *in vivo* or *ex vivo*

Panels **A** and **C** show *in vivo* muscle plantarflexion force (reported as plantarflexion torque and plantarflexion fatigue) in WT and KO female (**A**) and male (**C**) mice on a control or a low calcium diet, panels **B** and **D** show muscle electrophysiology parameters of CMAP, SMUP, and MUNE in WT and KO female (**B**) and male (**D**) mice, and panels **E** and **F** show *ex vivo* EDL functional measurement (reported as specific force frequency, maximum rate of contraction, maximum rate of relaxation, half-relaxation time, and % fatigue) in WT and KO female (**E**) and male (**F**) mice.

2-way ANOVA was performed. n= 4-5/group. As depicted here, red is female, and blue is male.

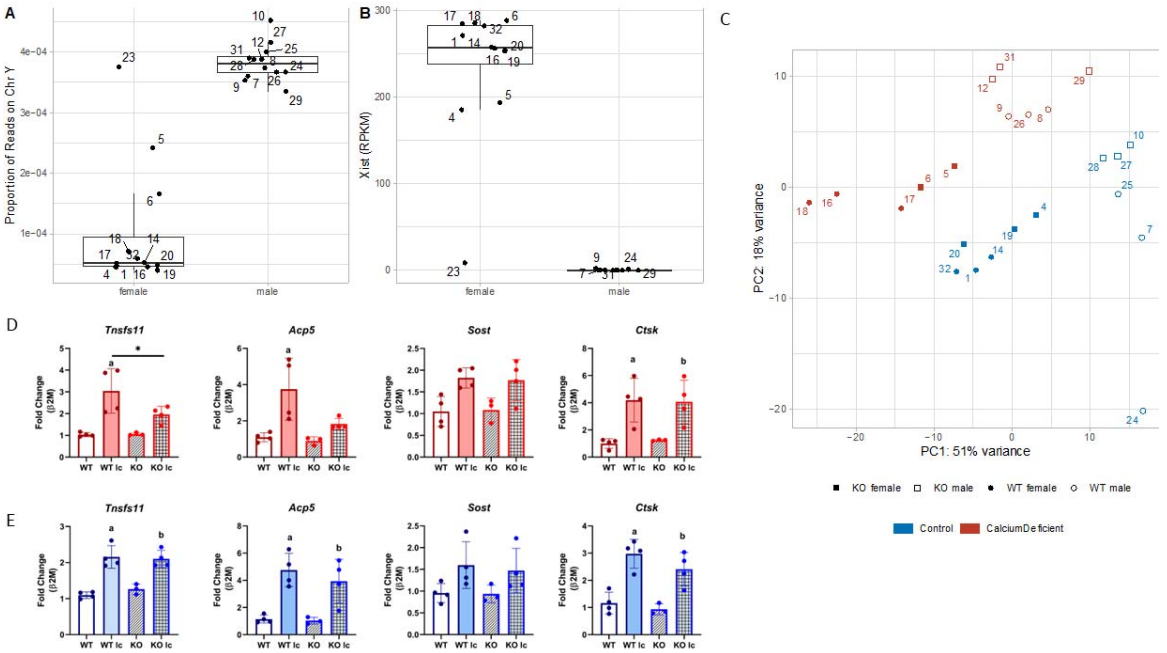

Supplementary Figure 3: Quality control and validation of RNA sequencing

Sanity check of data on the sample's sex. **A**: Boxplot of proportional of reads on chromosome Y. Male should have a higher value than female. **B**: Boxplot of RPKM of *Xist*. Males should have very low expression of *Xist*.

C: Scatter plot of PC1 and PC2 from Principal Component Analysis (PCA) of gene expression data.

D: qPCR analysis of *Tnsfs11*, *Acp5*, *Sost*, and *Ctsk* genes from osteocyte-enriched bone chips from female samples. n= 3-4/sample. Two-way ANOVA was performed for statistical analysis. Gene fold-change was normalized using β-2-microglobulin as the housekeeping gene. a= Significantly different from WT, b= Significantly different from KO, *= $p < 0.05$.

E: qPCR analysis of *Tnsfs11*, *Acp5*, *Sost*, and *Ctsk* genes from osteocyte-enriched bone chips from male samples. n= 3-4/sample. Two-way ANOVA was performed for statistical analysis. Gene fold-change was normalized using β-2-microglobulin as the housekeeping gene. a= Significantly different from WT, b= Significantly different from KO, *= $p < 0.05$.

Bone Parameters	Virgin		Lactation	
	WT	KO	WT	KO
Femoral cortical bone parameters				
Ct. B. Ar/T. Ar (%)	47.4 ± 1.2	48 ± 1	35.2 ± 1.8[a]	37.5 ± 1.8[b, c]
Ct. Th (mm)	0.18 ± 0.004	0.19 ± 0.005	0.13 ± 0.004[a]	0.14 ± 0.01[b, c]
Ps. Pm (mm)	5.16 ± 0.2	5.2 ± 0.06	5.18 ± 0.16	5.2 ± 0.14
Es. Pm (mm)	3.95 ± 0.1	4 ± 0.13	4.4 ± 0.11[a]	4.3 ± 0.09[b]
Marrow cavity area (mm^2)	0.93 ± 0.1	0.93 ± 0.04	1.16 ± 0.05[a]	1.13 ± 0.05[b]
Femoral trabecular bone parameters				
BV/TV (%)	3.7 ± 1	4.5 ± 0.8	3.1 ± 0.7	4 ± 1.1
Tb. Th (mm)	0.043 ± 0.002	0.044 ± 0.001	0.039 ± 0.002[a]	0.039 ± 0.001[b]
Tb. Sp (mm)	0.37 ± 0.05	0.36 ± 0.03	0.57 ± 0.15[a]	0.44 ± 0.09
Tb. N (1/mm)	0.85 ± 0.2	1.06 ± 0.2	0.8 ±0.2	1.04 ± 0.25

Bone parameters	Change	% Change	
		WT	KO
Cortical Bone Area Fraction	Decrease	26%	22% *
Cortical Thickness	Decrease	29%	24% *
Ultimate Force	Decrease	38%	31% *
Osteoclast Number/ bone parameter	Increase	141%	129%
TRAP-positive osteocytes	Increase	101%	175% *
Lacunar Area	Increase	26%	15% *
Serum RANKL	Increase	170%	80% *

Supplementary Table 1: FNDC5 KO mice femurs are partially resistant to lactation-induced bone loss.

Femoral cortical and trabecular bone parameters of WT and FNDC5 KO female virgin and lactation mice. n = 5-8/group. Data presented as mean ± standard deviation. a= significant compared to WT control, b= significant compared to KO control, c= significant compared to WT low Ca diet, 2-way ANOVA, significance <0.05, n= 8/group.

Percentage change in different bone and serum parameters in WT and FNDC5 KO female mice with lactation. *= p<0.05 compared to WT.

Bone Parameters	Female Normal Diet		Female Low Ca Diet		Male Normal Diet		Male Low Ca Diet	
	WT	KO	WT	KO	WT	KO	WT	KO
***Ex vivo* femur DXA**								
BMD (mg/cm^2)	75.4± 2.4	6.6± 1.5	65.4± 4.3[a]	71.4± 3.4 [c]	74.6± 1.5	78.3± 3[a]	68.2± 3	68.1± 2[b]
BMC (g)	0.03± 0.002	0.03± 0.001	0.024± 0.002[a]	0.027± 0.002 [b,c]	0.029± 0.002	0.032± 0.004	0.026± 0.002	0.025± 0.003[b]
Femoral cortical bone parameters								
Ct. B.Ar/T.Ar%	47.8± 1.6	48.4± 0.4	41.6± 1.1[a]	45.2± 1.4[b, c]	40.1± 1.4	43.6± 0.6[a]	38.3± 0.9	39.1± 1.2[b]
Ct. Th (mm)	0.2± 0.01	0.2± 0.01	0.15± 0.01[a]	0.17± 0.01[b, c]	0.15± 0.01	0.2± 0.01[a]	0.14± 0.01	0.14± 0.01[b]
Marrow Cavity Area	0.92 ± 0.04	0.86± 0.02	1.02 ± 0.06[a]	0.9 ± 0.02[c]	1.1 ± 0.04	1.03 ± 0.06[a]	1.2 ± 0.03	1.08 ± 0.03[c]
Femoral trabecular bone parameters								
BV/TV (%)	3.6 ± 1.2	4.3 ± 1	3.2 ± 1	3.9 ± 1	6.1 ± 1.1	8.7 ± 1.9	5.3 ± 1.2	6.4 ±0.6
Tb. Th (mm)	0.059± 0.002	0.059± 0.004	0.056± 0.002	0.055± 0.001	0.036 ± 0.001	0.035 ± 0.001	0.035±0. 001	0.035 ± 0.002
Tb. Sp (mm)	0.38 ± 0.03	0.35 ± 0.02	0.51 ± 0.12[a]	0.48 ± 0.08[b]	0.274 ± 0.025	0.235 ± 0.021	0.278 ± 0.027	0.265 ± 0.01
Tb. N (1/mm)	0.81 ± 0.2	0.95 ± 0.14	0.7 ± 0.02	0.91 ±0.13	1.7 ± 0.34	2.5[a] ± 0.5	1.5 ± 0.3	1.8 ± 0.1
Femoral mechanical properties								
Ultimate Force (N)	19± 1	19.4± 1.15	14.8± 0.7[a]	16.4± 0.5[b]	18.3± 1	17.6± 0.9	15± 1.3[a]	12.7± 1.5[b, c]
Stiffness (N/mm)	78.6± 3.2	79.1± 4.9	56.8± 5[a]	67± 4.3	76.7± 5.6	56.4± 4.75[a]	56± 10.2[a]	48.5± 4.9[b, c]
Energy to Failure (N)	2.9± 0.3	3.1± 0.6	1.8± 0.5[a]	2± 0.3[b]	3.6± 0.9	3.01± 0.6	2.5± 0.3[a]	2.35± 0.14

Supplementary Table 2: WT and FNDC5 KO female and male mice bone responds differently to a low-calcium diet

1043 Femoral BMD, BMC, cortical and trabecular bone parameters, and mechanical properties of
1044 4-5-month-old WT and KO female and male mice under a normal diet or a 2-week low calcium diet.
1045 n = 5/group. Data presented as mean ± standard deviation.
1046 a= significant compared to WT control, b= significant compared to KO control, c= significant
1047 compared to WT low Ca diet, 2-way ANOVA, significance <0.05, n= 4-5/group.
048

References

Andersson G, Ek-Rylander B, Hollberg K, Ljusberg-Sjölander J, Lång P, Norgård M, Wang Y, Zhang SJ. TRACP as an osteopontin phosphatase. J Bone Miner Res. 2003; 18(10):1912–1917.

Ardeshirpour L, Dumitru C, Dann P, Sterpka J, VanHouten J, Kim W, Kostenuik P, Wysolmerski J. OPG Treatment Prevents Bone Loss During Lactation But Does Not Affect Milk Production or Maternal Calcium Metabolism. Endocrinology. 2015; 156(8):2762–73.

Bao JF, She QY, Hu PP, Jia N, Li A. Irisin, a fascinating field in our times. Trends Endocrinol Metab. 2022; 33(9):601– 613.

Bélanger LF. Osteocytic osteolysis. Calcif Tissue Res. 1969; 4(1):1–12.

Body JJ, Terpos E, Tombal B, Hadji P, Arif A, Young A, Aapro M, Coleman R. Bone health in the elderly cancer patient: A SIOG position paper. Cancer Treat Rev. 2016; 51:46–53.

Bonewald L. Use it or lose it to age: A review of bone and muscle communication. Bone. 2019; 120:212–218.

Bonewald LF. The amazing osteocyte. J Bone Miner Res. 2011; 26(2):229–267.

Bostrom P, Wu J, Jedrychowski MP, Korde A, Ye L, Lo JC, Rasbach KA, Boström EA, Choi JH, Long JZ, Kajimura S, Zingaretti MC, Vind BF, Tu H, Cinti S, Højlund K, Gygi SP, Spiegelman BM. A PGC1-alpha-dependent myokine that drives brown-fat-like development of white fat and thermogenesis. Nature. 2012; 481(7382):463–471.

Bouxsein ML, Boyd SK, Christiansen BA, Guldberg RE, Jepsen KJ, Müller R. Guidelines for assessment of bone microstructure in rodents using micro- computed tomography. J Bone Miner Res. 2010; 25(7):1468–86.

Breese MR, Liu Y. NGSUtils: a software suite for analyzing and manipulating next- generation sequencing datasets. Bioinformatics. 2013; 29(4):494–500.

Brotto M, Bonewald L. Bone and muscle: Interactions beyond mechanical. Bone. 2015; 80:109–114.

Celi FS, Brown H. Adipose Tissue Plasticity: Hormonal and Environmental Manipulation, in Hormones. Spiegelman B, editor, Springer Copyright; 2017.

Colaianni G, Cuscito C, Mongelli T, Oranger A, Mori G, Brunetti G, Colucci S, Cinti S, Grano M. Irisin enhances osteoblast differentiation in vitro. Int J Endocrinol. 2014; p. 902186–902186.

Colaianni G, Cuscito C, Mongelli T, Pignataro P, Buccoliero C, Liu P, Lu P, Sartini L, Di Comite M, Mori G, Di Benedetto A, Brunetti G, Yuen T, Sun L, Reseland JE, Colucci S, New MI, Zaidi M, Cinti S, Grano M. The myokine irisin increases cortical bone mass. Proc Natl Acad Sci. 2015; 112(39):12157–62.

Colaianni G, Mongelli T, Cuscito C, Pignataro P, Lippo L, Spiro G, Notarnicola A, Severi I, Passeri G, Mori G, Brunetti Moretti B, Tarantino U, Colucci SC, Reseland JE, Vettor R, Cinti S, Grano M. Irisin prevents and restores bone loss and musc atrophy in hind-limb suspended mice. Sci Rep, 2017; 7(1): p. 2811.

Colaianni G, Grano M. Role of Irisin on the bone-muscle functional unit. Bonekey Rep, 2015; 4: p. 765.

Colucci SC, Buccoliero C, Sanesi L, Errede M, Colaianni G, Annese T, Khan MP, Zerlotin R, Dicarlo M, Schipani E, Kozloff KM, Grano M. Systemic Administration of Recombinant Irisin Accelerates Fracture Healing in Mice. Int J Mol Sci. 2019; p. 22–22.

Dallas SL, Prideaux M, Bonewald LF. The osteocyte: an endocrine cell ... and more. Endocr Rev. 2013; 34(5):658–90.

Dobin A, Davis CA, Schlesinger F, Drenkow J, Zaleski C, Jha S, Batut P, Chaisson M, Gingeras TR. STAR: ultrafa universal RNA-seq aligner. Bioinformatics. 2013; 29(1):15–21.

Dole NS, Yee CS, Mazur CM, Acevedo C, Alliston T. TGFβ Regulation of Perilacunar/Canalicular Remodeling Is Sexually Dimorphic. J Bone Miner Res. 2020; 35(8):1549-1561.

During A. Osteoporosis: A role for lipids. Biochimie. 2020; 178:49–55.

Erickson HP. Irisin and FNDC5 in retrospect: An exercise hormone or a transmembrane receptor? Adipocyte, 2013; 2(4): p. 289-93.

Essex AL, Huot JR, Deosthale P, Wagner A, Figueras J, Davis A, Damrath J, Pin F, Wallace J, Bonetto A, Plotkin LI. Triggering Receptor Expressed on Myeloid Cells 2 (TREM2) R47H Variant Causes Distinct Age- and Sex-Dependent Musculoskeletal Alterations in Mice. J Bone Miner Res. 2022; 37(7):1366–1381.

Estell EG, Le PT, Vegting Y, Kim H, Wrann C, Bouxsein ML, Nagano K, Baron R, Spiegelman BM, Rosen CJ. Irisin directly stimulates osteoclastogenesis and bone resorption in vitro and in vivo. Elife. 2020; p. 2020–2029.

Farley JR, Baylink DJ. Skeletal alkaline phosphatase activity as a bone formation index in vitro. Metabolism. 1986; 35(6):563–71.

Feng JQ, Ye L, Schiavi S. Do osteocytes contribute to phosphate homeostasis? Curr Opin Nephrol Hypertens. 2009; 18(4):285–91.

Geng W, Wright GL. Skeletal sensitivity to dietary calcium deficiency is increased in the female compared with the male rat. Can J Physiol Pharmacol. 2001; 79(5):379–85.

The Gene Ontology Resource: enriching a GOld mine TGO. Nucleic Acids Res. 2021; 49(D1):325–334.

Goltzman D. Studies on the mechanisms of the skeletal anabolic action of endogenous and exogenous parathyroid hormone. Arch Biochem Biophys. 2008; 473(2):218–242.

Gu Z. Complex heatmap visualization. iMeta, 2022; 1(3): p. e43.

Hamrick MW, Samaddar T, Pennington C, McCormick J. Increased muscle mass with myostatin deficiency improves gains in bone strength with exercise. J Bone Miner Res. 2006; 21(3):477–83.

Huot JR, Pin F, Essex AL, Bonetto A. MC38 Tumors Induce Musculoskeletal Defects in Colorectal Cancer. Int J Mol

Sci. 2021; 22(3).

Huot JR, Pin F, Chatterjee R, Bonetto A. PGC1α overexpression preserves muscle mass and function in cisplatin-induced cachexia. J Cachexia Sarcopenia Muscle. 2022; 13(5):2480–2491.

Islam MR, Valaris S, Young MF, Haley EB, Luo R, Bond SF, Mazuera S, Kitchen RR, Caldarone BJ, Bettio LEB, Christie BR, Schmider AB, Soberman RJ, Besnard A, Jedrychowski MP, Kim H, Tu H, Kim E, Choi SH, Tanzi RE, Spiegelman BM, Wrann CD. Exercise hormone irisin is a critical regulator of cognitive function. Nat Metab. 2021; (8):1058–1070.

Jahn K, Kelkar S, Zhao H, Xie Y, Tiede-Lewis LM, Dusevich V, Dallas SL, Bonewald LF. Osteocytes Acidify Their Microenvironment in Response to PTHrP In Vitro and in Lactating Mice In Vivo. J Bone Miner Res. 2017; 32(8):1761–1772.

Jähn-Rickert K, Zimmermann EA. Potential Role of Perilacunar Remodeling in the Progression of Osteoporosis and Implications on Age-Related Decline in Fracture Resistance of Bone. Curr Osteoporos Rep. 2021; 19(4):391–402.

Jo D, Song J. Irisin Acts via the PGC-1α and BDNF Pathway to Improve Depression-like Behavior. Clin Nutr Res. 2021; 10(4):292–302.

Johannesdottir F, Aspelund T, Reeve J, Poole KE, Sigurdsson S, Harris TB, Gudnason VG, Sigurdsson G. Similarities and differences between sexes in regional loss of cortical and trabecular bone in the mid-femoral neck: the AGES-Reykjavik longitudinal study. J Bone Miner Res. 2013; 28(10):2165–76.

Johnston CB, Dagar M. Osteoporosis in Older Adults. Med Clin North Am. 2020; 104(5):873–884.

Kalkwarf HJ. Lactation and maternal bone health. Adv Exp Med Biol. 2004; 554:101–115.

Kaplan MM. Alkaline phosphatase. N Engl J Med. 1972; 286(4):200–202.

Karsenty G, Mera P. Molecular bases of the crosstalk between bone and muscle. Bone. 2018; 115:43–49.

Kawao N, Moritake A, Tatsumi K, Kaji H. Roles of Irisin in the Linkage from Muscle to Bone During Mechanical Unloading in Mice. Calcif Tissue Int. 2018; 103(1):24–34.

Kim H, Wrann CD, Jedrychowski M, Vidoni S, Kitase Y, Nagano K, Zhou C, Chou J, Parkman VA, Novick SJ, Strutzenberg TS, Pascal BD, Le PT, Brooks DJ, Roche AM, Gerber KK, Mattheis L, Chen W, Tu H, Bouxsein ML, Griffin PR, Baron R, Rosen CJ, Bonewald LF, Spiegelman BM. Irisin Mediates Effects on Bone and Fat via alphaV Integrin Receptors. Cell. 2018; 175(7):17–17.

Kitase Y, Vallejo JA, Gutheil W, Vemula H, Jähn K, Yi J, Zhou J, Brotto M, Bonewald LF. β-aminoisobutyric Acid, l-BAIBA, Is a Muscle-Derived Osteocyte Survival Factor. Cell Rep. 2018; 22(6):1531–1544.

Korta P, Pocheć E, Mazur-Biały A. Irisin as a Multifunctional Protein: Implications for Health and Certain Diseases Medicina (Kaunas), 2019; 55(8).

Kovacs CS. Calcium and bone metabolism in pregnancy and lactation. The Journal of clinical endocrinology and metabolism. 2001; (6):86–86.

142 **Kumssa DB**, Joy EJ, Ander EL, Watts MJ, Young SD, Walker S, Broadley MR. Dietary calcium and zinc deficiency risks are
143 decreasing but remain prevalent. Sci Rep, 2015; 5: p. 10974.

144 **Kurapaty SS**, Hsu WK. Sex-Based Difference in Bone Healing: A Review of Recent Preclinical Literature. Curr
145 Rev Musculoskelet Med. 2022.

146 **Lee HJ**, Lee JO, Kim N, Kim JK, Kim HI, Lee YW, Kim SJ, Choi JI, Oh Y, Kim JH, Suyeon-Hwang, Park SH, Kim HS.
147 Irisin, a Novel Myokine, Regulates Glucose Uptake in Skeletal Muscle Cells via AMPK. Mol Endocrinol. 2015; 29(6):873–81.

148 **Liao Y**, Smyth GK, Shi W. featureCounts: an efficient general purpose program for assigning sequence reads
149 to genomic features. Bioinformatics. 2014; 30(7):923–953.

150 **Liu Q**, Lei L, Yu T, Jiang T, Kang Y. Effect of Brain-Derived Neurotrophic Factor on the Neurogenesis and
151 Osteogenesis in Bone Engineering. Tissue Eng Part A. 2018; 24:1283–1292.

152 **Love MI**, Huber W, Anders S. Moderated estimation of fold change and dispersion for RNA-seq data with
153 DESeq2. Genome Biol. 2014; 15(12):550–550.

154 **Lu D**, Demissie S, Horowitz NB, Gower AC, Lenburg ME, Alekseyev YO, Hussein AI, Bragdon B, Liu Y, Daukss D, Page JM,
155 Webster MZ, Schlezinger JJ, Morgan EF, Gerstenfeld LC. Temporal and Quantitative Transcriptomic Differences Define Sexual
156 Dimorphism in Murine Postnatal Bone Aging. JBMR Plus, 2022; 6(2): p. e10579.

157 **Luo X**, Li J, Zhang H, Wang Y, Shi H, Ge Y, Yu X, Wang H, Dong Y. Irisin promotes the browning of white adipocytes
158 tissue by AMPKα1 signaling pathway. Res Vet Sci. 2022; 152:270–276.

159 **Ma Y**, Qiao X, Zeng R, Cheng R, Zhang J, Luo Y, Nie Y, Hu Y, Yang Z, Zhang J, Liu L, Xu W, Xu CC, Xu L. Irisin
160 promotes proliferation but inhibits differentiation in osteoclast precursor cells. Faseb j. 2018; p. 201700983–201700983.

161 **Maak S**, Norheim F, Drevon CA, Erickson HP. Progress and Challenges in the Biology of FNDC5 and Irisin. Endocr
162 Rev. 2021; 42(4):436–456.

163 **Matikainen N**, Pekkarinen T, Ryhänen EM, Schalin-Jäntti C. Physiology of Calcium Homeostasis: An Overview.
164 Endocrinol Metab Clin North Am. 2021; 50(4):575–590.

165 **Melville KM**, Robling AG, Meulen MCVD. In vivo axial loading of the mouse tibia. Methods Mol Biol. 2015;
166 1226:99–115.

167 **Mo C**, Zhao R, Vallejo J, Igwe O, Bonewald L, Wetmore L, Brotto M. Prostaglandin E2 promotes proliferation of
168 skeletal muscle myoblasts via EP4 receptor activation. Cell Cycle. 2015; 14(10):1507–1523.

169 **Moreno-Layseca P**, Icha J, Hamidi H, Ivaska J. Integrin trafficking in cells and tissues. Nat Cell Biol. 2019;
170 21(2):122– 132.

171 **Mu A**, Wales TE, Zhou H, Draga-Coletă SV, Gorgulla C, Blackmore KA, Mittenbühler MJ, Kim CR, Bogoslavski D,
172 Zhang Q, Wang ZF, Jedrychowski MP, Seo HS, Song K, Xu AZ, Sebastian L, Gygi SP, Arthanari H, Dhe-Paganon S, Griffin PR,
173 Engen JR, Spiegelman BM. Irisin acts through its integrin receptor in a two-step process involving extracellular Hsp90α.

Mol Cell. 2023; 83(11):1903–1920.

Muruganandan S, Sinal CJ. The impact of bone marrow adipocytes on osteoblast and osteoclast differentiation. IUBMB Life. 2014; 66(3):147–155.

Nakashima T, Hayashi M, Fukunaga T, Kurata K, Oh-Hora M, Feng JQ, Bonewald LF, Kodama T, Wutz A, Wagner EF, Penninger JM, Takayanagi H. Evidence for osteocyte regulation of bone homeostasis through RANKL expression. Nat Med. 2011; 17(10):1231–1235.

Ono T, Hayashi M, Sasaki F, Nakashima T. RANKL biology: bone metabolism, the immune system, and beyond. Inflamm Regen, 2020; 40: p. 2.

Osipov B, Paralkar MP, Emami AJ, Cunningham HC, Tjandra PM, Pathak S, Langer HT, Baar K, Christiansen BA. Sex differences in systemic bone and muscle loss following femur fracture in mice. J Orthop Res. 2022; (4):878–890.

Perakakis N, Triantafyllou GA, Fernández-Real JM, Huh JY, Park KH, Seufert J, Mantzoros CS. Physiology and role of irisin in glucose homeostasis. Nat Rev Endocrinol. 2017; 13(6):324–337.

Pin F, Prideaux M, Huot JR, Essex AL, Plotkin LI, Bonetto A, Bonewald LF. Non-bone metastatic cancers promote osteocyte-induced bone destruction. Cancer Lett. 2021; 520:80–90.

Pin F, Jones AJ, Huot JR, Narasimhan A, Zimmers TA, Bonewald LF, Bonetto A. RANKL Blockade Reduces Cachexia and Bone Loss Induced by Non-Metastatic Ovarian Cancer in Mice. J Bone Miner Res. 2022; 37(3):381–396.

Posa F, Colaianni G, Di Cosola M, Dicarlo M, Gaccione F, Colucci S, Grano M, Mori G. The Myokine Irisin Promotes Osteogenic Differentiation of Dental Bud-Derived MSCs. Biology. 2021;(4).

Qi JY, Yang LK, Wang XS, Wang M, Li XB, Feng B, Wu YM, Zhang K, Liu SB. Irisin: A promising treatment for neurodegenerative diseases. Neuroscience. 2022; 498:289–299.

Qing H, Ardeshirpour L, Pajevic PD, Dusevich V, Jähn K, Kato S, Wysolmerski J, Bonewald LF. Demonstration of osteocytic perilacunar/canalicular remodeling in mice during lactation. J Bone Miner Res. 2012; 27(5):1018–1047.

Qing H, Bonewald LF. Osteocyte remodeling of the perilacunar and pericanalicular matrix. International Journal of Oral Science. 2009.

Robling AG, Bonewald LF. The Osteocyte: New Insights. Annu Rev Physiol. 2020; 82:485– 506.

Rosen CJ, Bouxsein ML. Mechanisms of disease: is osteoporosis the obesity of bone? Nat Clin Pract Rheumatol. 2006; 2(1):35–43.

Saedi A, Bermeo S, Plotkin L, Myers DE, Duque G. Mechanisms of palmitate-induced lipotoxicity in osteocytes. Bone. 2019; 127:353–359.

Saedi A, Chen L, Phu S, Vogrin S, Miao D, Ferland G, Gaudreau P, Duque G. Age-Related Increases in Marrow Fat Volumes have Regional Impacts on Bone Cell Numbers and Structure. Calcif Tissue Int. 2020; 107(2):126–134.

Schwartz AV. Marrow fat and bone: review of clinical findings. Front Endocrinol (Lausanne), 2015; 6: p. 40.

Sharma A, Michels LV, Pitsillides AA, Greeves J, Plotkin LI, Cardo V, Sims NA, Clarkin CE. Sexing Bones: Improving Transparency of Sex Reporting to Address Bias Within Preclinical Studies. J Bone Miner Res. 2023; 38(1):5–13.

Shimonty A, Bonewald LF, Pin F. Role of the Osteocyte in Musculoskeletal Disease. Curr Osteoporos Rep. 2023; 21(3):303–310.

Silver IA, Murrills RJ, Etherington DJ. Microelectrode studies on the acid microenvironment beneath adherent macrophages and osteoclasts. Exp Cell Res. 1988; 175(2):266–76.

Styner M, Pagnotti GM, Galior K, Wu X, Thompson WR, Uzer G, Sen B, Xie Z, Horowitz MC, Styner MA, Rubin C, Rubin J.Exercise Regulation of Marrow Fat in the Setting of PPARμ Agonist Treatment in Female C57BL/6 Mice. Endocrinology. 2015; 156(8):2753–61.

Team RC. R: A Language and Environment for Statistical Computing. 2022, R Foundation for Statistical Computing. In: 2022.

Temiyasathit S, Jacobs CR. Osteocyte primary cilium and its role in bone mechanotransduction. Ann N Y Acad Sci. 2010; 1192:422–430.

Teti A, Zallone A. Do osteocytes contribute to bone mineral homeostasis? Osteocytic osteolysis revisited. Bone. 2009; 44(1):11–17.

Tsourdi E, Jähn K, Rauner M, Busse B, Bonewald LF. Physiological and pathological osteocytic osteolysis. J Musculoskelet Neuronal Interact. 2018; 18(3):292–303.

Tsourdi E, Anastasilakis AD, Hofbauer LC, Rauner M, Lademann F. Irisin and Bone in Sickness and in Health: A Narrative Review of the Literature. J Clin Med. 2022; (22):11–11.

Uda Y, Azab E, Sun N, Shi C, Pajevic PD. Osteocyte Mechanobiology. Curr Osteoporos Rep, 2017; 15(4): p. 318-325.

Wang H, Zhao YT, Zhang S, Dubielecka PM, Du J, Yano N, Chin YE, Zhuang S, Qin G, Zhao TC. Irisin plays a pivotal role to protect the heart against ischemia and reperfusion injury. J Cell Physiol. 2017; 232(12):3775–3785.

Wickham H. GGPLOT2: Elegant Graphics for Data Analysis. New York: Springer-Verlag; 2016.

Wrann CD, White JP, Salogiannnis J, Laznik-Bogoslavski D, Wu J, Ma D, Lin JD, Greenberg ME, Spiegelman BM. Exercise induces hippocampal BDNF through a PGC-1α/FNDC5 pathway. Cell Metab. 2013; 18(5):649–59.

Wu T. clusterProfiler 4.0: A universal enrichment tool for interpreting omics data. Innovation (Camb), 2021; 2(3): p. 100141.

Wysolmerski JJ. The evolutionary origins of maternal calcium and bone metabolism during lactation. J Mammary Gland Biol Neoplasia. 2002; 7(3):267–76.

Wysolmerski JJ. Osteocytic osteolysis: time for a second look? Bonekey Rep, 2012; 1: p. 229.

Wysolmerski JJ. Osteocytes remove and replace perilacunar mineral during reproductive cycles. Bone. 2013; 54(2):230–236.

Xin C, Liu J, Zhang J, Zhu D, Wang H, Xiong L, Lee Y, Ye J, Lian K, Xu C, Zhang L, Wang Q, Liu Y, Tao L. Irisin improves fatty acid oxidation and glucose utilization in type 2 diabetes by regulating the AMPK signaling pathway. Int J Obes. 2016; 40(3):443–51.

Xiong J, Piemontese M, Onal M, Campbell J, Goellner JJ, Dusevich V, Bonewald L, Manolagas SC, O'Brien CA. Osteocytes, not Osteoblasts or Lining Cells, are the Main Source of the RANKL Required for Osteoclast Formation in Remodeling Bone. PLoS One. 2015; 10(9):138189– 138189.

Xiong J, O'Brien CA. Osteocyte RANKL: new insights into the control of bone remodeling. J Bone Miner Res. 2012; 27(3):499–505.

Yeung DK, Griffith JF, Antonio GE, Lee FK, Woo J, Leung PC. Osteoporosis is associated with increased marrow fat content and decreased marrow fat unsaturation: a proton MR spectroscopy study. J Magn Reson Imaging. 2005; 22(2):279–85.

YoultenSE, Kemp JP, Logan JG, Ghirardello EJ, Sergio CM, Dack MRG, Guilfoyle SE, Leitch VD, Butterfield NC, Komla-Ebri D, Chai RC, Corr AP, Smith JT, Mohanty ST, Morris JA, McDonald MM, Quinn JMW, McGlade AR, Bartonicek N, Jansson M, Hatzikotoulas K, Irving MD, Beleza-Meireles A, Rivadeneira F, Duncan E, Richards JB, Adams DJ, Lelliott CJ, Brink R, Phan TG, Eisman JA, Evans DM, Zeggini E, Baldock PA, Bassett JHD, Williams GR, Croucher PI. Osteocyte transcriptome mapping identifies a molecular landscape control- ling skeletal homeostasis and susceptibility to skeletal disease. Nat Commun. 2021; 12(1):2444–2444.

Young MF, Valaris S, Wrann CD. A role for FNDC5/Irisin in the beneficial effects of exercise on the brain and in neurodegenerative diseases. Prog Cardiovasc Dis. 2019; 62(2):172– 178.

Zhang D, Bae C, Lee J, Lee J, Jin Z, Kang M, Cho YS, Kim JH, Lee W, Lim SK. The bone anabolic effects of irisin are through preferential stimulation of aerobic glycolysis. Bone. 2018; 114:150–160.

Zhang H, Wu X, Liang J, Kirberger M, Chen N. Irisin, an exercise-induced bioactive peptide beneficial for health promotion during aging process. Ageing Res Rev. 2022; 80:101680–101680.

Zhang Y, Li R, Meng Y, Li S, Donelan W, Zhao Y, Qi L, Zhang M, Wang X, Cui T, Yang LJ, Tang D. Irisin stimulates browning of white adipocytes through mitogen-activated protein kinase p38 MAP kinase and ERK MAP kinase signaling. Diabetes. 2014; 63(2):514–539.

Zhu J, Li J, Yao T, Li T, Chang B, Yi X. Analysis of the role of irisin receptor signaling in regulating osteogenic/adipogenic differentiation of bone marrow mesenchymal stem cells. Biotechnol Genet Eng Rev. 2023; p. 1–24.